Supporting Information

Molecular dyads with non-fused electron acceptor backbones for single-component organic solar cells

Wei Wang, Yuan Gao, Yao Wu, Xinrong Yang, Zhihao Chen, Zeng Chen, Tao Wang, Rui Sun, Qiang Wu, Xiaotao Hao, Haiming Zhu, Sergey *Ponomarenko, Yuriy Luponosov, and Jie Min**

Contents:

1. Experimentation section

Materials. 4,7-dibromo-5,6-difluorobenzo[c][1,2,5]thiadiazole was purchased from Energy Chemical and used as received. BDT-3T-R was synthesized in our lab according to our previously reported work.[1] Solvents were dried and distilled from appropriate drying agents prior to use.

Synthesis of Tz-IC2F

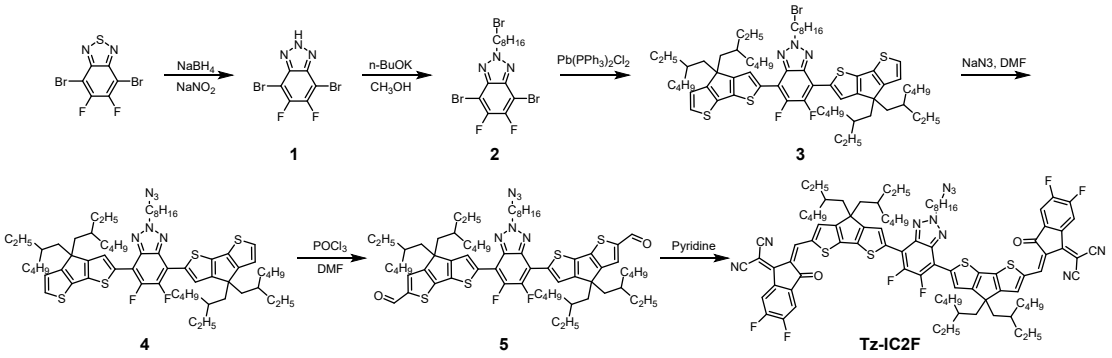

Scheme S1. Synthesis of Tz-IC2F.

4,7-Dibromo-5,6-difluorobenzo[c][1,2,5]thiadiazole (1.98 g, 6.00 mmol) and $zinc_{(dust)}$ (3.92 g, 60.0 mmol) were dissolved in acetic acid (30 mL) and water (7 mL) under argon protection and stirred for 2 h at 90 °C. After removing $zinc_{(dust)}$ through filtration, the reaction mixture was extracted with diethyl ether and washed with 5% NaOH for three times. The organic layer was then dried over anhydrous $MgSO_4$ and filtered and concentrated under reduced pressure. 3,6-Dibromo-4,5-difluorobenzene-1,2-diamine was used crude upon concentration immediately in the next step without further purification to avoid fast decomposition.

3,6-Dibromo-4,5-difluorobenzene-1,2-diamine was dissolved in acetic acid (10 mL) and water (5 mL). A solution of sodium nitrite ($NaNO_2$) (537.4 mg, 7.79 mmol) dissolved in water (2 mL) was slowly added to the reaction mixture and stirred at room temperature for 1 h, followed by ultrasonication of the mixtures until providing the pale

brown solid precipitate in the solution. Finally, the reaction mixture was cooled to 0 ℃ and stirred for additional 30 min to have solid precipitate effectively formed. The solid was then filtered and washed with water thoroughly to give a pale brown solid **compound 1** for two steps. (1.41 g, 75%). The compound was used in the next reaction without further purification.

Compound 1 (4.53 g, 14.5 mmol), 1,8-dibromooctane (3.94 g, 14.5 mmol) and Potassium tert-butoxide (4.60 g, 41mmol) were dissolved in methanol (50 ml) and stirred for 24 h at 90 ℃ under argon atmosphere. After reaction was completed, the reaction was quenched by water. The reaction mixture was then extracted by dichloromethane and washed with water. The crude product was then concentrated in vacuo, followed by column chromatography (petroleum ether/DCM 1/1, *v*/*v*) to give a white solid **compound 2** (4.37 g. 60%). ^{1}H-NMR (600 MHz, Chloroform-d): δ(ppm): 4.77 (t, J = 7.2 Hz, 2H), 3.40 (t, J = 7.2 Hz, 2H), 2.10-2.20 (m, 2H), 1.81-1.88 (m, 2H), 1.30-1.45 (m, 8H).

A mixture of **compound 2** (1.78 g, 3.53 mmol), (4,4-bis(2-ethylhexyl)-4H-cyclopenta[1,2- b:5,4-b']dithiophen-2-yl)trimethylstannane (5.0 g, 8.84 mmol), and $Pd(PPh_3)_2Cl_2$ (115.6 mg, 0.10 mmol) in dry toluene (50 mL) was stirred at 110 °C under argon for 12 h. After cooling to room temperature, the mixture was poured into a solution of KF and extracted with DCM (50 mL × 3). The combined organic layer was dried over anhydrous Na_2SO_4, filtered, and evaporated to dryness. The residue was purified via column chromatography on silica gel (petroleum ether/ DCM, 7/1, *v*/*v*) to afford **compound 3** (2.67 g, 66%) as an orange oil. ^{1}H-NMR (600 MHz, Chloroform-d): δ(ppm): 8.10-8.14 (m, 2H), 7.21 (s, 1H), 7.20 (s, 1H), 6.96-7.00 (m, 2H), 4.83 (t, J = 7.2 Hz, 2H), 3.39 (td, J = 6.6 Hz, J = 0.6 Hz, 2H), 2.18-2.25 (m, 2H), 1.83-2.05 (m, 10H), 1.41-1.50 (m, 6H), 1.33-1.39 (m, 2H), 1.23-1.31 (m, 4H), 0.82-1.06 (m, 32H), 0.73-0.77 (m, 8H), 0.59-0.71 (m, 16H).

A mixture of **compound 3** (1.22 g, 1.06 mmol) and sodium azide (78 mg, 1.20 mmol)

in DMF (20 mL) was stirred at 110 ℃ under argon for 12 h. After cooling to room temperature, the mixture was poured into water and extracted with DCM (50 mL × 3). The combined organic layer was dried over anhydrous Na_2SO_4, filtered, and evaporated to dryness. The residue was purified via column chromatography on silica gel (petroleum ether/ DCM, 7/1, *v*/*v*) to afford **compound 4** (1.06 g, 91%) as an orange oil. ^{1}H-NMR (600 MHz, Chloroform-d): δ(ppm): 8.10-8.14 (m, 2H), 7.21 (s, 1H), 7.20 (s, 1H), 6.96-7.00 (m, 2H), 4.84 (t, J = 7.2 Hz, 2H), 3.25 (t, J = 7.2 Hz, 2H), 2.18-2.25 (m, 2H), 1.89-2.07 (m, 8H), 1.58-1.66 (m, 2H), 1.20-1.50 (m, 10H), 0.83-1.06 (m, 32H), 0.72-0.78 (m, 8H), 0.60-0.68 (m, 16H).

To a solution of **compound 4** (1.06 mg, 0.96 mmol) in anhydrous DMF (20 mL), phosphorus oxychloride (0.90 mL, 9.60 mmol) was added dropwise under the protection of argon at 0°C. After stirring at 0°C for 1 h, the mixture was heated to 90°C and stirred overnight. The mixture was poured into water (100 mL) to quench the reaction and extracted with extracted with DCM (10 mL × 3). The combined organic layer was dried over anhydrous Na_2SO_4, filtered, and evaporated to dryness. The residue was purified via column chromatography on silica gel (DCM/ethyl acetate, 250/0.5, *v*/*v*) to afford **compound 5** (0.95 g, 85%) as a deep orange oil. ^{1}H-NMR (400 MHz, Chloroform-d): δ(ppm): 9.86 (s, 2H), 8.16-8.20 (m, 2H), 7.59-7.63 (m, 2H), 4.85 (t, J = 7.2 Hz, 2H), 3.23 (t, J = 6.6 Hz, 2H), 2.17-2.27 (m, 2H), 1.92-2.11 (m, 8H), 1.54-1.62 (m, 2H), 1.30-1.51 (m, 8H), 0.87-1.08 (m, 34H), 0.69-0.75 (m, 8H), 0.58-0.69 (m, 16H).

To a solution of **compound 5** (0.35 g, 0.30 mmol), 2-(5,6-difluoro-3-oxo-2,3-dihydro-1Hinden-1-ylidene)malononitrile (0.28 g, 1.20 mmol) and pyridine (0.4 mL) in $CHCl_3$ (20 mL) was heated at 60 °C overnight. After cooling to room temperature, the mixture was concentrated to 5 mL and poured into methanol (50 mL) and then filtered. The residue was purified via column chromatography on silica gel (petroleum ether/DCM, 1:2, *v*/*v*) to afford **Tz-IC2F** (0.42 g, 88%) as a dark solid. ^{1}H-NMR (400 MHz, Chloroform-d): δ(ppm): 8.92 (s, 2H), 8.50-8.56 (m, 2H), 8.23-8.27 (m, 2H), 7.63-7.74

(m, 4H), 4.89 (t, J = 7.2 Hz, 2H), 3.27 (t, J = 6.8 Hz, 2H), 2.20-2.31 (m, 2H), 1.95-2.15 (m, 8H), 1.55-1.66 (m, 2H), 1.35-1.53 (m, 8H), 1.24-1.33 (m, 2H), 0.85-1.06 (m, 34H), 0.69-0.77 (m, 12H), 0.60-0.68 (m, 12H). ^{13}C-NMR (101 MHz, Chloroform-d): δ(ppm): 186.17, 165.39, 160.38, 158.56, 158.23, 155.33, 155.23, 153.58, 153.49, 148.69, 148.56, 146.99, 146.86, 140.26, 140.17, 139.66, 138.48, 138.29, 138.19, 137.55, 136.66, 134.63, 125.50, 125.47, 119.92, 115.08, 114.93, 114.76, 114.71, 112.64, 112.52, 111.20, 68.41, 57.37, 54.27, 51.55, 43.42, 43.25, 43.16, 35.65, 35.59, 34.57, 34.55, 34.14, 30.04, 29.84, 29.18, 29.13, 28.96, 28.62, 28.54, 27.71, 27.39, 26.83, 26.66, 22.93, 22.88, 14.21, 14.09, 10.74. HRMS (MALDI-TOF): Calcd. for $C_{90}H_{94}F_6N_{10}O_2S_4$, exact m/z ($M^+$) = 1588.6734; Found: 1588.6348.

Synthesis of SW1

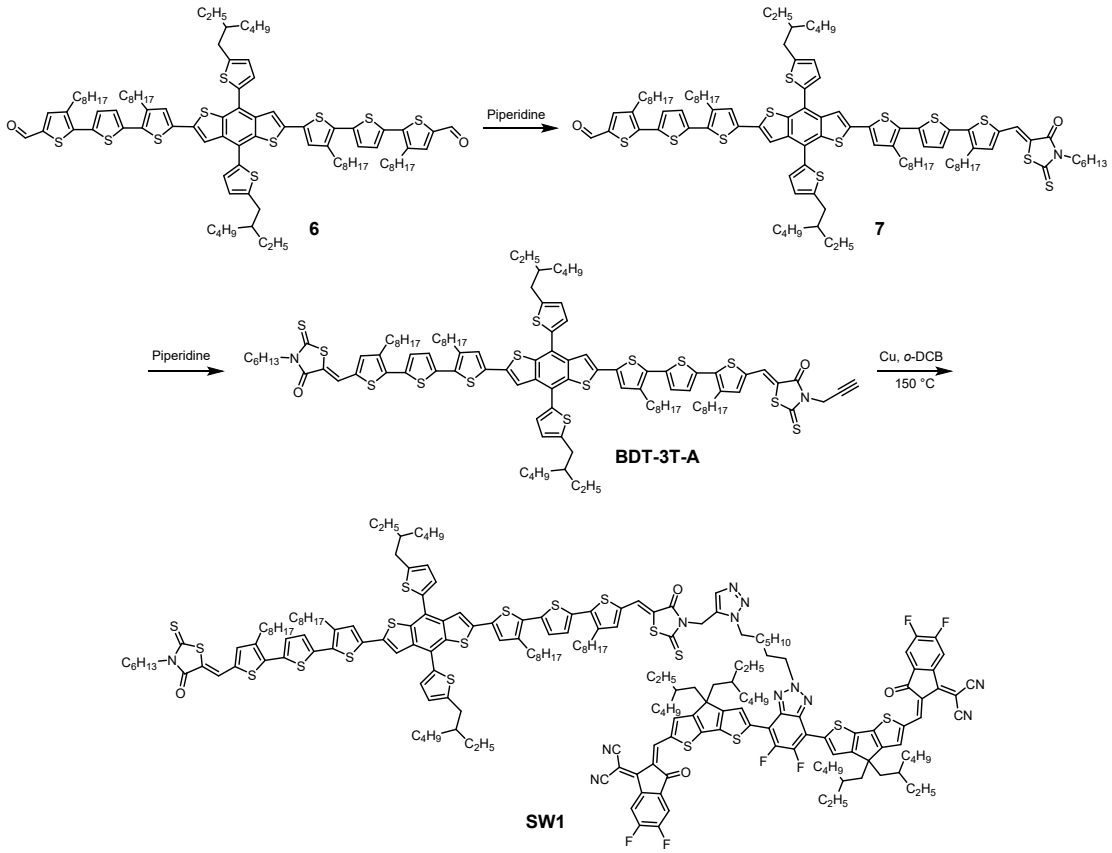

Scheme S2. Synthesis of SW1.

Compound 6 (0.65 g, 0.41 mmol) was dissolved in a dry chloroform (400 mL) and 0.4

mL piperidine was added under nitrogen, and resulting solution was heated to reflux. Then, 3-hexylrhodanine (98 mg, 0.45 mmol) was divided into five parts, and added into the reaction solution every 6 hours. The reaction mixture was cooled down to room temperature, poured into methanol. Solid was filtered and washed several times with methanol. The residue was purified via column chromatography on silica gel (chloroform) to afford **compound 7** (0.40 g, 55%) as a dark solid. Then, the intermediate **products 7** was dissolved in a dry chloroform (50 mL) and 0.4 mL piperidine was added under nitrogen. Then, 3-(2-propynyl)-rhodanine (57 mg, 0.34 mmol) was added and resulting solution was heated to reflux and stirred for 12 hours. The reaction mixture was cooled down to room temperature, poured into methanol. Solid was filtered and washed several times with methanol. After silica gel column chromatography ($CHCl_3$), a dark black solid compound, **BDT-3T-A** (0.36 g, 84%), was obtained. ^{1}H-NMR (600 MHz, Chloroform-d): δ(ppm): 7.72-7.77 (m, 1H), 7.68-7.71 (m, 1H), 7.52-7.58 (m, 2H), 7.28-7.34 (m, 2H), 7.12-7.20 (m, 4H), 7.00-7.10 (m, 4H), 6.92-6.97 (m, 2H), 4.78-4.87 (m, 2H), 4.00-4.11 (m, 2H), 2.87-2.96 (m, 4H), 2.68-2.83 (m, 8H), 2.23-2.26 (m, 1H), 1.72-1.80 (m, 2H), 1.63-1.72 (m, 8H), 1.23-1.52 (m, 64H), 0.98-1.03 (m, 6H), 0.93-0.97 (m, 6H), 0.82-0.91 (m, 15H). ^{13}C-NMR (125 MHz, Chloroform-d): δ(ppm): 192.19, 190.81, 167.46, 166.31, 145.96, 140.88, 140.04, 139.46, 138.59, 137.75, 137.54, 137.29, 137.25, 136.83, 135.58, 134.69, 134.55, 130.44, 130.38, 128.29, 127.86, 127.27, 127.13, 126.05, 125.69, 125.49, 124.77, 123.24, 120.41, 119.63, 119.11, 75.94, 72.03, 44.83, 41.50, 34.38, 33.53, 32.55, 31.89, 31.34, 30.42, 30.22, 30.19, 29.71, 29.61, 29.51, 29.47, 29.33, 29.30, 28.98, 26.93, 26.46, 25.85, 23.11, 22.69, 22.52, 14.27, 14.13, 14.02, 11.01.. HRMS (MALDI-TOF): Calcd. for $C_{107}H_{134}N_2O_2S_{14}$, exact m/z ($M^+$) = 1926.6535; Found: 1926.8911.

A mixture of **Tz-IC2F** (0.12 g, 0.076 mmol), **BDT-3T-A** (0.15 g, 0.076 mmol) and Cu (48 mg, 0.76 mmol) in 1,2-dichlorobenzene (40 mL) was stirred at 150 ℃ under argon for 4 hours. After cooling to room temperature, the mixture was concentrated to 2 mL and poured into methanol (20 mL) and then filtered. The residue was purified via column chromatography on silica gel (chloroform/methanol, 250:0.5, *v*/*v*) to afford

SW1 (0.18 g, 71%) as a dark solid. ^{1}H-NMR (600 MHz, Chloroform-d): δ(ppm): 8.88 (s, 2H), 8.42-8.53 (m, 2H), 8.21-8.27 (m, 2H), 7.58-7.74 (m, 7H), 7.46-7.56 (m, 2H), 7.28-7.36 (m, 2H), 7.10-7.20 (m, 4H), 7.04-7.08 (m, 2H), 6.93-6.98 (m, 2H), 5.38-5.44 (m, 2H), 4.81-4.88 (m, 2H), 4.33-4.40 (m, 2H), 4.02-4.10 (m, 2H), 2.87-2.96 (m, 4H), 2.68-2.82 (m, 8H), 2.18-2.27 (m, 2H), 1.89-2.13 (m, 12H), 1.62-1.79 (m, 12H), 1.22-1.55 (m, 74H), 0.93-1.10 (m, 44H), 0.84-0.91 (m, 15H), 0.71-0.83 (m, 12H), 0.62-0.69 (m, 12H). ^{13}C-NMR (125 MHz, Chloroform-d): δ(ppm): ^{13}C NMR (151 MHz, $CDCl_3$) δ 192.31, 191.67, 186.10, 167.59, 167.05, 165.35, 165.30, 160.37, 158.48, 158.14, 155.26, 155.16, 153.52, 153.41, 148.49, 146.93, 146.81, 146.13, 146.10, 141.49, 141.08, 141.04, 140.30, 140.16, 140.05, 139.67, 139.60, 138.68, 138.15, 137.90, 137.77, 137.67, 137.50, 137.40, 137.35, 136.89, 136.60, 136.55, 135.71, 135.59, 135.25, 134.92, 134.84, 134.56, 130.63, 130.49, 128.47, 128.03, 127.29, 127.27, 126.21, 126.08, 126.05, 125.62, 125.56, 125.42, 124.90, 123.62, 123.35, 120.58, 119.94, 119.88, 119.20, 115.00, 114.87, 114.75, 112.61, 112.47, 111.17, 68.32, 57.28, 54.21, 50.45, 44.97, 43.33, 43.21, 43.18, 43.08, 41.62, 39.53, 35.67, 35.62, 34.56, 34.54, 34.50, 34.15, 32.68, 32.05, 32.01, 31.47, 30.55, 30.50, 30.35, 30.29, 29.99, 29.96, 29.92, 29.87, 29.86, 29.80, 29.75, 29.73, 29.69, 29.67, 29.63, 29.59, 29.46, 29.43, 29.11, 28.98, 28.92, 28.63, 28.55, 27.75, 27.40, 27.07, 26.59, 26.50, 25.96, 23.24, 22.95, 22.91, 22.83, 22.82, 22.65, 14.40, 14.27, 14.26, 14.23, 14.15, 14.12, 14.10, 11.14, 10.83, 10.76. HRMS (MALDI-TOF): Calcd. for $C_{197}H_{228}F_6N_{12}O_4S_{18}$, exact m/z ($M^+$) = 3519.1414; Found: 3519.6625.

Synthesis of SW2

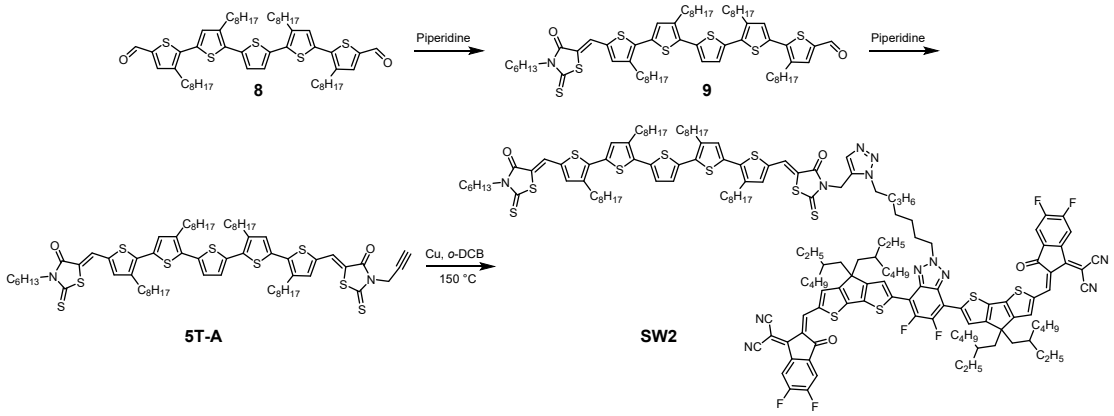

Scheme S3. Synthesis of SW2.

Compound 8 (1.11 g, 1.21 mmol) was dissolved in a dry chloroform (400 mL) and 0.4 mL piperidine was added under nitrogen, and resulting solution was heated to reflux. Then, 3-hexylrhodanine (0.32 g, 1.45 mmol) was divided into five parts, and added into the reaction solution every 6 hours. The reaction mixture was cooled down to room temperature, poured into methanol. Solid was filtered and washed several times with methanol. The residue was purified via column chromatography on silica gel (chloroform) to afford **compound 9** (0.82 g, 61%) as a dark solid. Then, the intermediate **products 9** was dissolved in a dry chloroform (50 mL) and 0.4 mL piperidine was added under nitrogen. Then, 3-(2-propynyl)-rhodanine (0.16 g, 0.96 mmol) was added and resulting solution was heated to reflux and stirred for 12 hours. The reaction mixture was cooled down to room temperature, poured into methanol. Solid was filtered and washed several times with methanol. After silica gel column chromatography ($CHCl_3$), a dark black solid compound, **5T-A** (0.67 g, 72%), was obtained. ^{1}H-NMR (600 MHz, Chloroform-d): δ(ppm): 7.83 (s, 1H), 7.77 (s, 1H), 7.24 (s, 1H), 7.22 (s, 1H), 7.15 (s, 2H), 7.09-7.13 (m, 2H), 4.87 (d, J = 2.4 Hz, 2H), 4.10 (t, J = 7.5 Hz, 2H), 2.74 (t, J = 7.8 Hz, 8H), 2.25 (t, J = 2.4 Hz, 1H), 1.64-1.75 (m, 12H), 1.39-1.46 (m, 8H), 1.25-1.39 (m, 36H), 0.85-0.91 (15H). ^{13}C-NMR (125 MHz, Chloroform-d): δ(ppm): ^{13}C NMR (151 MHz, $CDCl_3$) δ 192.42, 191.04, 167.69, 166.55, 141.32, 141.24, 140.67, 140.66, 140.26, 139.67, 138.02, 137.53, 135.97, 135.84, 135.29, 134.97, 133.13, 132.97, 132.54, 132.30, 130.21, 130.07, 126.62, 126.58,

125.99, 125.05, 120.64, 119.87, 76.05, 72.20, 45.01, 33.72, 32.05, 32.01, 31.49, 30.72, 30.38, 30.36, 29.79, 29.65, 29.61, 29.55, 29.53, 29.46, 29.40, 27.10, 26.60, 22.82, 22.65, 14.27, 14.16. HRMS (MALDI-TOF): Calcd. for $C_{69}H_{92}N_2O_2S_9$, exact m/z (M^+) = 1268.4645; Found: 1268.4901.

A mixture of **Tz-IC2F** (0.13 g, 0.082 mmol), **5T-A** (0.10 g, 0.082 mmol) and Cu (52 mg, 0.82 mmol) in 1,2-dichlorobenzene (40 mL) was stirred at 150 ℃ under argon for 4 hours. After cooling to room temperature, the mixture was concentrated to 2 mL and poured into methanol (20 mL) and then filtered. The residue was purified via column chromatography on silica gel (chloroform/methanol, 250:0.5, *v*/*v*) to afford **SW2** (0.14 g, 58%) as a dark solid. ^{1}H-NMR (600 MHz, Chloroform-d): δ(ppm): 8.91 (s, 2H), 8.47-8.57 (m, 2H), 8.18-8.27 (m, 2H), 7.59-7.82 (m, 7H), 7.16-7.22 (m, 2H), 7.04-7.22 (m, 4H), 5.43 (s, 2H), 4.88 (t, J = 6.9 Hz, 2H), 4.35 (t, J = 6.9 Hz, 2H), 4.10 (t, J = 7.8 Hz, 2H), 2.74-2.84 (m, 8H), 2.19-2.28 (m, 2H), 1.98-2.13 (m, 8H), 1.90-1.95 (m, 2H), 1.63-1.75 (m, 12H), 1.23-1.50 (m, 56H), 0.92-1.05 (m, 32H), 0.82-0.91 (m, 15H), 0.71-0.76 (m, 12H), 0.61-0.69 (m, 12H). ^{13}C-NMR (125 MHz, Chloroform-d): δ(ppm): ^{13}C NMR (151 MHz, $CDCl_3$) δ 192.39, 191.78, 186.19, 167.67, 167.13, 165.39, 160.39, 158.55, 158.20, 155.30, 155.19, 153.56, 153.47, 148.70, 148.57, 147.01, 146.87, 141.48, 141.30, 141.23, 140.65, 140.32, 140.30, 140.14, 139.64, 138.39, 138.25, 138.16, 137.88, 137.53, 136.64, 136.59, 135.97, 135.79, 135.28, 134.96, 134.61, 134.57, 133.12, 132.92, 132.52, 132.28, 130.14, 130.04, 126.59, 126.54, 125.71, 125.49, 125.02, 123.54, 120.64, 119.98, 119.93, 115.05, 114.91, 114.76, 112.64, 112.52, 111.17, 68.37, 57.29, 54.26, 50.44, 45.00, 43.40, 43.23, 43.15, 39.56, 35.66, 35.61, 34.55, 34.13, 32.03, 32.00, 30.70, 30.35, 30.32, 30.00, 29.84, 29.78, 29.65, 29.60, 29.55, 29.52, 29.52, 29.45, 29.39, 28.98, 28.94, 28.62, 28.54, 27.72, 27.39, 27.08, 26.59, 26.53, 22.93, 22.88, 22.82, 22.81, 22.64, 14.26, 14.25, 14.22, 14.15, 14.10, 14.08, 10.81, 10.76.. HRMS (MALDI-TOF): Calcd. for $C_{159}H_{186}F_6N_{12}O_4S_{13}$, exact m/z ($M^+$) = 2858.1027; Found: 2858.0660.

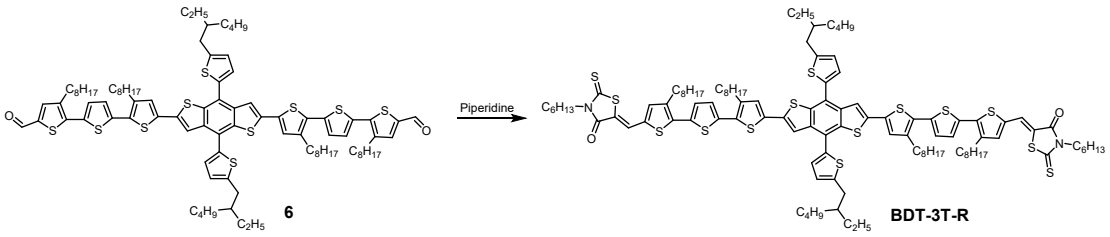

Scheme S4. Synthesis of BDT-3T-R.

Synthesis of 5T-R

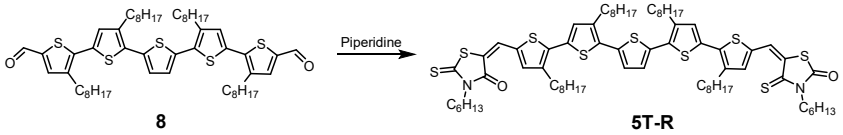

Scheme S5. Synthesis of 5T-R.

Compound 8 (0.31 g, 0.34 mmol) was dissolved in a dry chloroform (400 mL) and 0.4 mL piperidine was added under nitrogen, and resulting solution was heated to reflux. Then, 3-hexylrhodanine (0.32 g, 1.45 mmol) was added and resulting solution was heated to reflux and stirred for 12 hours. The reaction mixture was cooled down to room temperature, poured into methanol. Solid was filtered and washed several times with methanol. After silica gel column chromatography ($CHCl_3$), a dark black solid compound, **5T-R** (0.38 g, 85%), was obtained. ^{1}H-NMR (600 MHz, Chloroform-d): δ(ppm): 7.76 (s, 2H), 7.22 (s, 2H), 7.14 (s, 2H), 7.19 (s, 2H), 4.10 (t, J = 7.8 Hz, 4H), 2.81 (t, J = 7.8 Hz, 8H), 1.65-1.74 (m, 12H), 1.39-1.46 (m, 8H), 1.23-1.38 (m, 44H), 0.83-0.91 (m, 18H). ^{13}C-NMR (125 MHz, Chloroform-d): δ(ppm): ^{13}C NMR (151 MHz, $CDCl_3$) δ 192.41, 167.68, 141.22, 140.63, 139.69, 137.52, 135.90, 135.27, 133.09, 132.34, 130.06, 126.56, 125.05, 120.62, 45.00, 32.05, 32.01, 31.49, 30.72, 30.38, 29.85, 29.79, 29.66, 29.61, 29.55, 29.54, 29.46, 29.41, 27.09, 26.60, 22.83, 22.65, 14.27, 14.16.. HRMS (MALDI-TOF): Calcd. for $C_{72}H_{102}N_2O_2S_9$, exact m/z (M^+) = 1314.5428; Found: 1314.5585.

Instruments and Characterization

Material characterization

^{1}HNMR spectra were obtained by JNM ECZ400 and AVANCE NEO 600 spectrometer using $CDCl_3$ as solution and tetramethylsilane (TMS) as internal standard in parts per million (ppm, δ) units. Mass spectrum was collected on a Bruker BIFLEX III MALDI-TOF mass spectrometer. UV-vis spectra were recorded on a Lambda 25 spectrophotometer. Electrochemical measurements were carried out at room temperature in an acetonitrile solution of 0.1 mol L^{-1} Bu_4NPF_6 using ferrocene (-4.8 eV) as standard reference, with a computer-controlled CHI660C electrochemical workstation. All CV curves were measured by films cast from $CHCl_3$ solution on the glassy carbon electrode with Pt wire as the counter electrode and Ag/AgCl as reference electrode. Differential Scanning Calorimetry (DSC) results were obtained by using a DSC 4000 Perkin Elmer analyzer under purified nitrogen gas flow with a 10 °C min^{-1} heating rate.

Device Fabrication and Testing

The solar cell devices were fabricated with a conventional structure of Glass/ITO/PEDOT:PSS (40nm)/sole photoactive layer/PNDIT-F3N/Ag. Pre-patterned ITO coated glass substrates (purchased from South China Science ＆Technology Company Limited) washed with methylbenzene, deionized water, acetone and isopropyl alcohol in an ultrasonic bath for 15 min each. After blow-dried by high-purity nitrogen, All ITO substrates are cleaned in ultraviolet ozone cleaning system for 15 minutes. Subsequently, a thin layer of PEDOT: PSS (Xi'an Polymer Light Technology Corp 4083) was deposited through spin-coating at 3500 rpm for 30s on pre-cleaned ITO-coated glass from a PEDOT: PSS aqueous solution and d annealed at 150 °C for 15 min in atmospheric air. Then the single active layer was spin-coated in ambient atmosphere from a solution of 12 mg mL^{-1} in chloroform onto the PEDOT: PSS layer at a varied coating speed for controlling the morphology and thickness of photoactive layer. Then methanol solution of PNDIT-F3N at a concentration of 1.0 $mgml^{-1}$ was

spin-coated onto the active layer at 3000 rpm for 30s. To complete the fabrication of the devices, 100 nm of Ag were thermally evaporated through a mask under a vacuum of ~6×10^{-6} mbar. The active area of the devices was 4 mm^2. The current-voltage characteristics of the solar cells were measured under AM 1.5G irradiation on an Enli Solar simulator (100 mW cm^{-2}). Before each test, the solar simulator was calibrated with a standard single-crystal Si solar cell (made by Enli Technology Co., Ltd., Taiwan, calibrated by The National Institute of Metrology (NIM) of China).

Instruments and Characterization

AFM measurements were performed with a Nano Wizard 4 atomic force microscopy (JPK Inc. Germany) in Qi mode to observe the surface morphologies of the pristine films and blends films deposited on glass substrates. 2D GIWAXS measurements: The 2D GIWAXS measurement was performed at the small and wide angle X-ray scattering beamline at the Australian Synchrotron. A Pilatus 1M 2-dimensional detector with 0.172 mm × 0.172 mm active pixels was utilized in integration mode. The detector was positioned approximately 300 mm downstream from the sample location. The precise sample-to-detector distance was determined with a silver behenate standard. 11 KeV incident X-ray with approximately a 0.25 mm × 0.1 mm spot was used to provide large enough q space. The 2-dimensional raw data was reduced and analyzed with a modified version of Nika. 1D GIWAXS patterns shown have been corrected to represent real Q_z and Q_{xy} axes with the consideration of missing wedge. Critical incident angle was determined by the maximized scattering intensity from sample scattering with negligible contribution from underneath layer scattering. The shallow incident angle scattering was collected at 0.02°, which renders the incident X-ray as an evanescent wave along the top surface of thin films.

SCLC measurement: Single carrier devices were fabricated and the dark current-voltage characteristics measured and analyzed in the space charge limited current (SCLC) regime following the references. For the hole-only and electron-only devices,

SCLC is described by[6,7]:

$$J_{scl} = \frac{9}{8}\varepsilon_0\varepsilon_r\mu\frac{V_{in}^2}{L^3}exp(\frac{0.89\times\beta}{\sqrt{L}}\sqrt{V}) \quad (1)$$

And

$$C \equiv \frac{N_t\beta^4 J}{2\varepsilon_0\varepsilon_r\mu N_c}exp(\frac{A}{kT}) \quad (2)$$

Where J_{SCL} is the current density, ε_0 is the permittivity of free-space, ε_r is the relative dielectric constant of the active layer, μ is charge carrier mobility, L is the thickness of the device and V_{in} is the voltage dropped across the sample. N_c is the effective density of conduction-band states, N_t is the effective density of trapping states, A is the energy of trapping level below conduction-band edge, k is Boltzmann's constant and T is the absolute temperature. The reported mobility data are average values over the two cells of each sample at a given film composition.

2. **Supporting figures and tables**

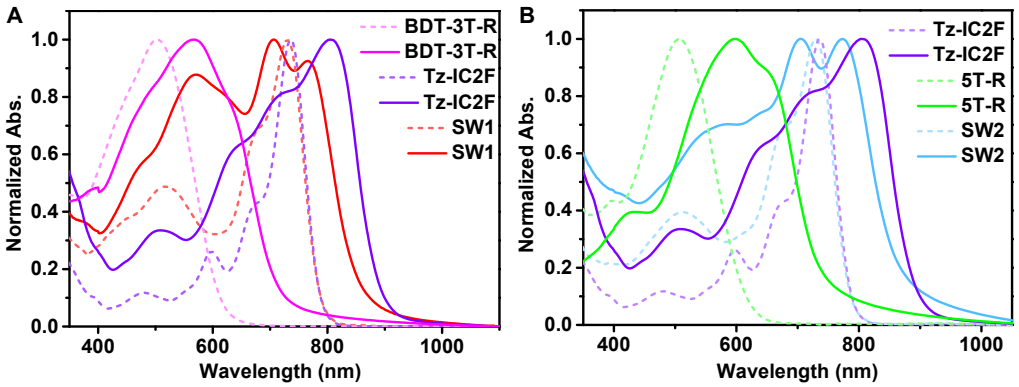

Figure S1. Normalized UV-vis absorption spectra of (A) BDT-3T-R, Tz-IC2F, and SW1 and (B) Tz-IC2F, 5T-R, and SW2 in dilute CF solution (dashed) and in the corresponding thin films (solid).

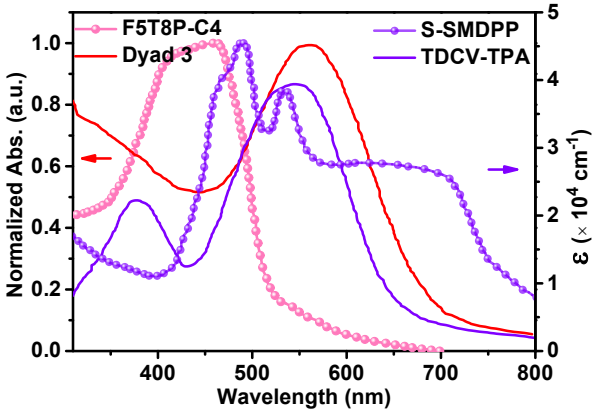

Figure S2. Normalized UV-vis absorption spectra of F5T8P-C4 and Dyad 3 in solution and the absorption coefficients of S-SMDPP and TDCV-TPA films.

Table S1. Summary of optical properties of relevant photovoltaic materials.

Compound	$\lambda_{max}^{sol, a)}$ (nm)	$\varepsilon^{solution}$ ($\times 10^5$ M^{-1} cm^{-1})	$\lambda_{max}^{film,c)}$ (nm)	$\lambda_{edge}^{film, c)}$ (nm)	ε^{film} ($\times 10^4$ cm^{-1})	$E_g^{opt, g)}$ (eV)
TDCV-TPA	--	--	546.2	653.2	4.0	1.90
F5T8P-C4	446.6	--	463.9	515.1	--	2.41
Dyad 3	522.0[b)]	--	562.0[d)]	678.4[d)]	--	1.83
S-SMDPP	530.5[e)]	--	488.7[f)]	838.0[f)]	4.6	1.48
SW1	730.0	2.13	706.0	855.5	7.7	1.45
SW2	730.0	2.03	773.0	858.1	5.8	1.44

[a)]Measured in chloroform solution; [b)]Measured in CH_2Cl_2 solution; [c)]Cast from chloroform solution; [d)]Cast from CH_2Cl_2 solution; [e)]Measured in *o*-DCB solution; [f)]Cast from *o*-DCB solution; [g)]Bandgap estimated from the onset wavelength (λ_{edge}) of the optical absorption: $E_g^{opt} = 1240/\lambda_{edge}$.

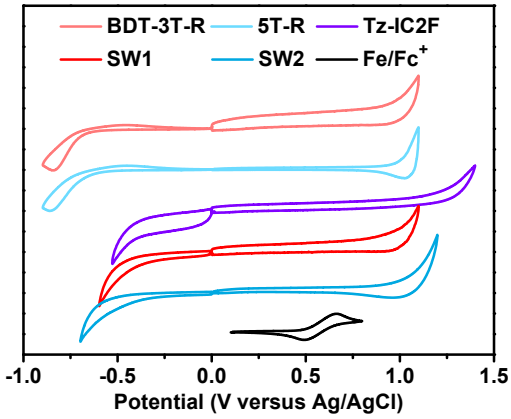

Figure S3. Cyclic voltammogram (CV) curves of BDT-3T-R, 5T-R, Tz-IC2F, SW1 and SW2 on Pt electrode in 0.1 M Bu_4NPF_6, CH_3CN solution, the black line shows the CV of ferrocene/ferrocenium (Fe/Fc^+) couple used as an internal reference.

Table S2. The parameters of optical properties and electronic energy levels of BDT-3T-R, 5T-R, Tz-IC2F, SW1 and SW2.

Compound	$\lambda_{max}^{sol, a)}$ (nm)	$\lambda_{max}^{film, b)}$ (nm)	$\lambda_{edge}^{film, b)}$ (nm)	$E_g^{opt, c)}$ (eV)	HOMO[d)] (eV)	LUMO[d)] (eV)	E_g^{cv} (eV)
BDT-3T-R	502.0	568.0	711.8	1.74	-5.20	-3.53	1.67
5T-R	507.0	598.0	740.5	1.67	-5.23	-3.56	1.67
Tz-IC2F	736.0	804.0	890.2	1.39	-5.46	-3.80	1.66
SW1	730.0	706.0	855.5	1.45	-5.23	-3.78	1.45
SW2	730.0	773.0	858.1	1.44	-5.30	-3.77	1.53

[a)]Measured in chloroform solution; [b)]Cast from chloroform solution; [c)]Bandgap estimated from the onset wavelength (λ_{edge}) of the optical absorption: $E_g^{opt} = 1240/\lambda_{edge}$; [d)]Measured by electrochemical cyclic voltammetry.

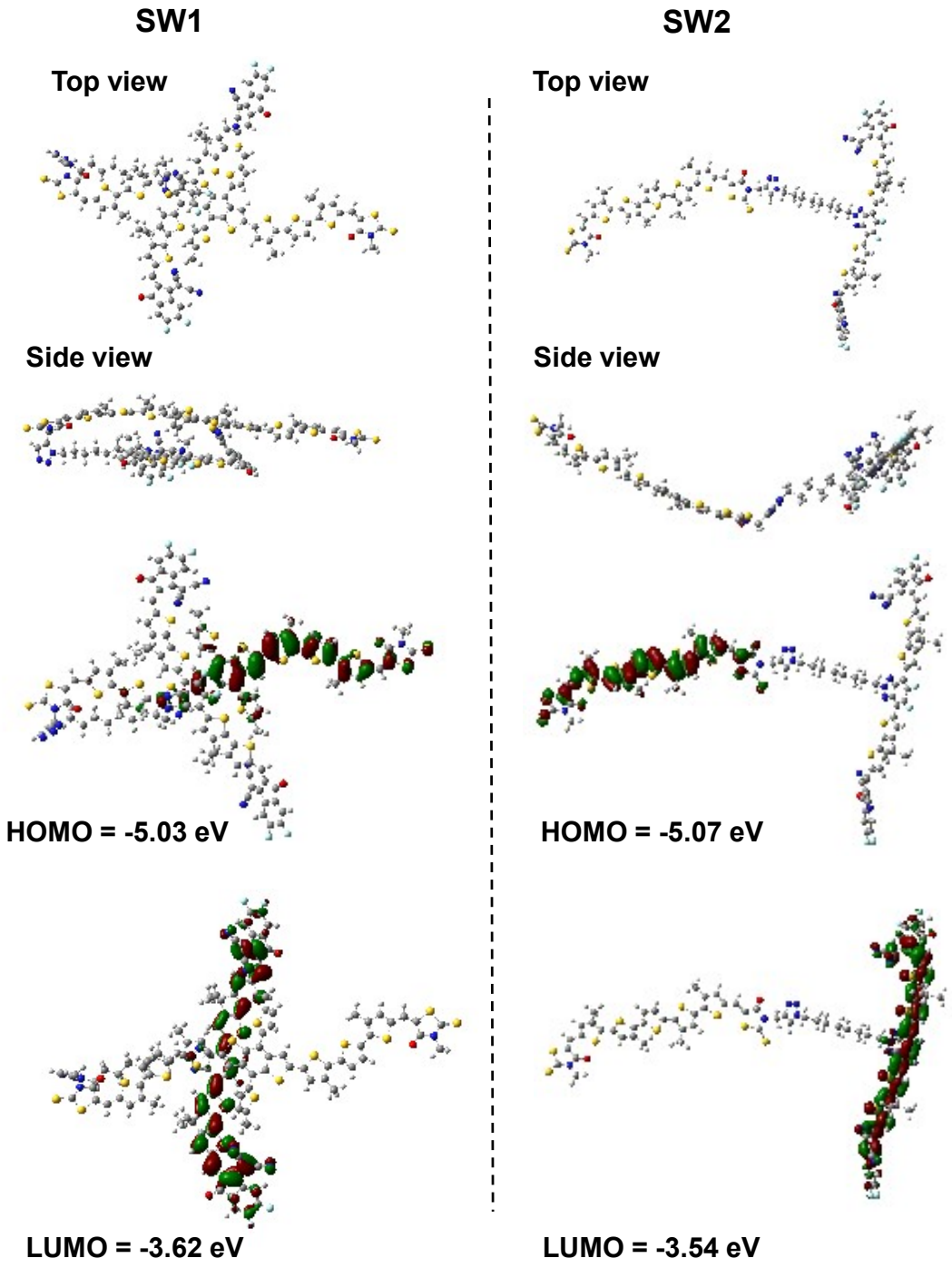

Figure S4. Molecular geometry, HOMO and LUMO energy levels of SW1 and SW2 calculated by DFT/B3L YP/6-31G (d, p) with methyl groups in relacing alkyl substituents to simplify the calculations.

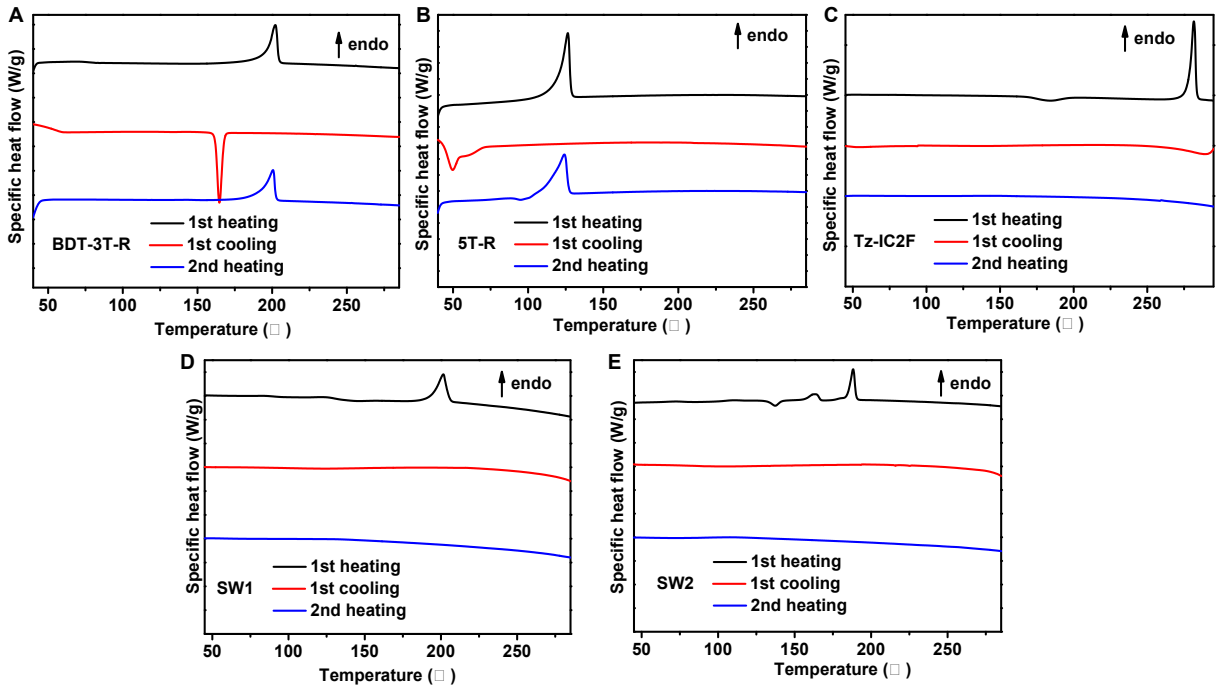

Figure S5. Thermal behavior of A) BDT-3T-R, B) 5T-R, C) Tz-IC2F, D) SW1 and E) SW2.

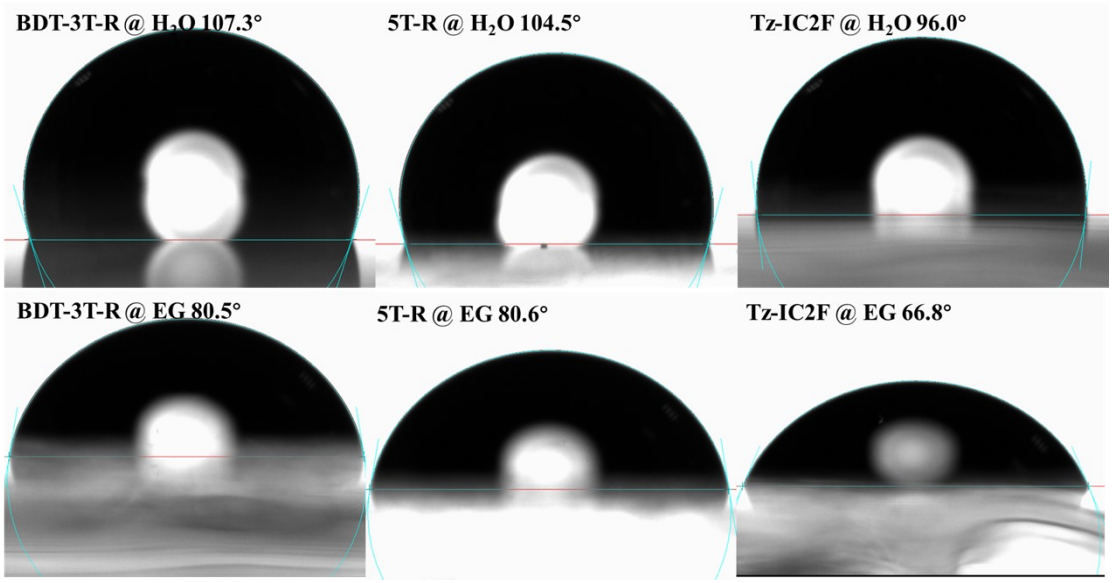

Figure S6. Photographs of water and ethylene glycol (EG) droplets on the top surfaces of pristine BDT-3T-R, 5T-R and Tz-IC2F films.

Table S3. Contact angles of water and ethylene glycol (EG) and their parameters of the donors BDT-3T-R, 5T-R and the acceptor Tz-IC2F.

Organic layer	Contact angel [H_2O] (˚)	Contact angel [EG] (˚)	Surface energy (mN m^{-1})	$\chi^{a)}$ [Tz-IC2F, A]
BDT-3T-R	107.3	80.5	39.25	0.13
5T-R	104.5	80.6	30.25	1.28
Tz-IC2F	96.0	66.8	43.97	n/a

[a)]The Flory-Huggins interaction parameter based on the surface tension data formula, $\chi = (\sqrt{\gamma(D)} - \sqrt{\gamma(A)})^2$.

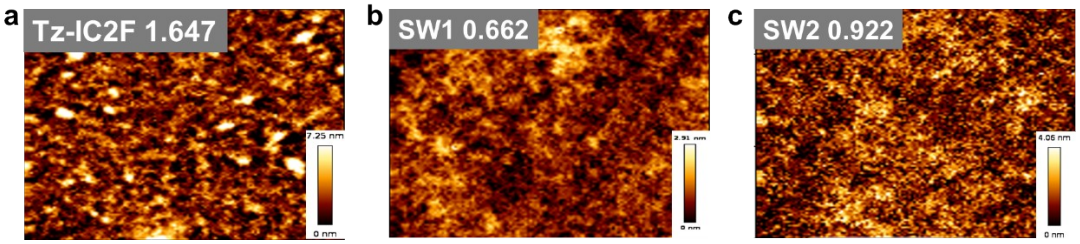

Figure S7. AFM images of Tz-IC2F, SW1 and SW2.

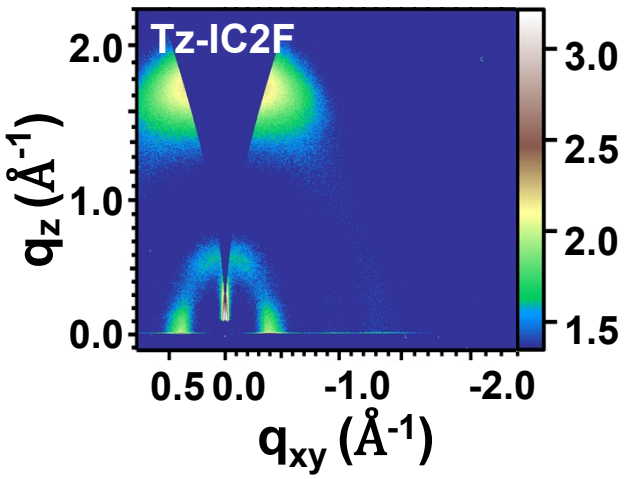

Figure S8. 2D GIWAXS patterns of Tz-IC2F.

Table S4. Detailed GIWAXS parameters for Tz-IC2F, SW1 and SW2 films

Materials	(100) Peak Position ($Å^{-1}$)	(100) *d*-spacing (Å)	(010) Peak Position ($Å^{-1}$)	(010) *d*-spacing (Å)	FWHM of (010) peak ($Å^{-1}$)	Coherence length of (010) stacking (Å)
Tz-IC2F	0.40	15.85	1.75	3.58	0.30	20.59
SW1	0.33	19.10	1.71	3.68	0.53	11.86
SW2	0.36	17.22	1.71	3.68	0.58	10.92

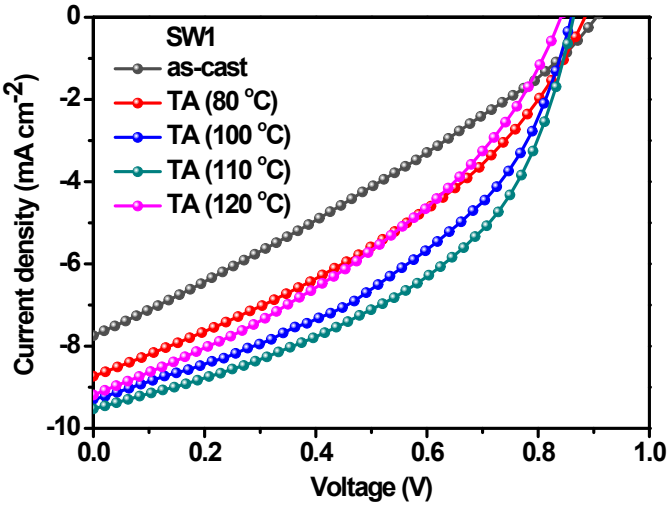

Figure S9. *J-V* curve statistics of SW1 under different thermal annealing temperatures. The annealing time is 10 minutes.

Table S5. Photovoltaic parameters of the SW1-based devices processed with different TA temperature. The annealing time is 10 minutes.

Temperature (°C)	V_{OC} (V)	J_{SC} (mA/cm^2)	FF (%)	PCE (%)
As-cast	0.902 (0.895 ± 0.06)[a)]	7.75 (7.51 ± 0.22)	29.7 (28.8 ± 0.7)	2.08 (1.94 ± 0.12)
80	0.884 (0.875 ± 0.12)	8.73 (8.55 ± 0.18)	36.6 (36.2 ± 0.5)	2.82 (2.71 ± 0.10)
100	0.859 (0.853 ± 0.05)	9.29 (9.21 ± 0.10)	42.5 (42.2 ± 0.4)	3.39 (3.32 ± 0.06)
110	0.863 (0.860 ± 0.03)	9.50 (9.42 ± 0.07)	46.1 (45.5 ± 0.5)	3.78 (3.69 ± 0.08)
120	0.843 (0.835 ± 0.07)	9.18 (9.05 ± 0.12)	36.8 (36.5 ± 0.2)	2.85 (2.76 ± 0.06)

[a)]The average values with standard deviations were obtained from eight devices.

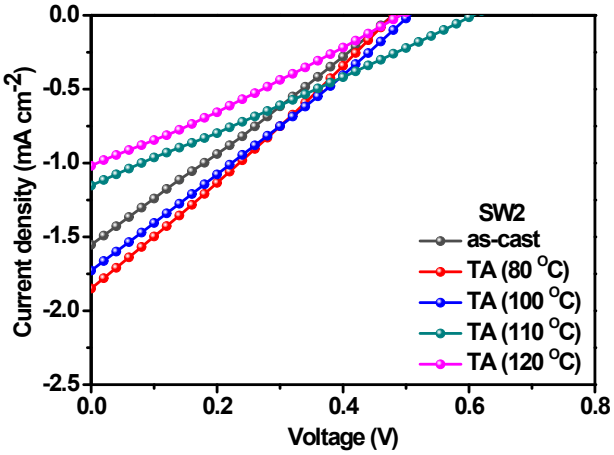

Figure S10. *J-V* curve statistics of SW2 under different thermal annealing temperatures. The annealing time is 10 minutes.

Table S6. Photovoltaic parameters of the SW2-based devices processed with different TA temperature. The annealing time is 10 minutes.

Temperature (°C)	V_{OC} (V)	J_{SC} (mA/cm^2)	FF (%)	PCE (%)
As-cast	0.484 (0.478 ± 0.15)[a)]	1.54 (1.47 ± 0.08)	26.5 (25.5 ± 0.8)	0.20 (0.19 ± 0.01)
80	0.478 (0.470 ± 0.07)	1.85 (1.79 ± 0.05)	26.6 (26.3 ± 0.1)	0.24 (0.21 ± 0.02)
100	0.530 (0.512 ± 0.15)	1.83 (1.82 ± 0.0.02)	26.2 (26.0 ± 0.2)	0.25 (0.24 ± 0.01)
110	0.606 (0.605 ± 0.01)	1.15 (1.12 ± 0.02)	26.2 (25.9 ± 0.3)	0.18 (0.17 ± 0.01)
120	0.491 (0.490 ± 0.02)	1.02 (1.02 ± 0.03)	26.8 (26.1 ± 0.25)	0.13 (0.12 ± 0.01)

[a)]The average values with standard deviations were obtained from eight devices.

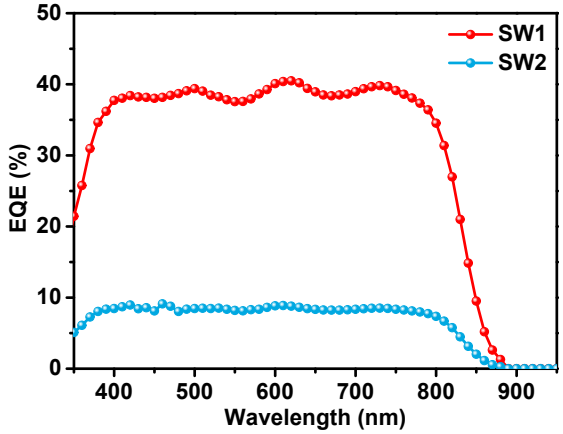

Figure S11. EQE spectra of SW1and SW2 devices.

Table S7. The photovoltaic parameters of non-fullerene SCOSCs based on molecular active materials.

Active material	V_{OC} (V)	J_{SC} (mA cm^{-2})	FF	PCE(%)	Reference
TDCV-TPA	0.76	1.70	0.27	0.40	2
F3T4-Hp	0.90	3.16	0.25	0.70	3
F4T6-Hp	0.86	4.05	0.34	1.18	3
F5T8-Hp	0.87	4.49	0.38	1.50	3
F3T4-epP	0.84	2.33	0.22	0.42	4
F4T6-epP	0.85	4.92	0.32	1.32	4
F5T8-epP	0.88	5.90	0.35	1.75	4
F5T8P-C2	1.00	4.30	0.43	1.86	5
F5T8P-C4	1.04	4.82	0.47	2.33	5
F5T8P-C6	0.96	4.6	0.46	2.04	5
OPV-NDI	0.91	0.31	0.28	0.08	6
BTT 1	0.55	1.55	0.45	0.38	7
BTT 2	0.38	1.22	0.38	0.35	7
BTT 3	0.51	2.36	0.45	0.54	7
BTT 4	0.37	1.05	0.37	0.12	7
BTT 5	0.40	0.98	0.40	0.15	7
BTT 6	0.49	1.52	0.40	0.30	7
SMDPP	0.68	5.62	0.45	1.73	8
S-SMDPP	0.73	8.03	0.43	2.52	8
SF-SMDPP	0.83	6.08	0.4	2.04	8
BTID-0F	0.99	2.61	0.62	1.61	9
ITIC-OE	0.88	0.8	0.33	0.23	10
ITIC	0.83	0.07	0.35	0.02	10
BTI	0.76	3.98	0.31	0.94	11
TPA	1.13	1.70	0.243	0.47	11
N(Ph-2T-DCV-Et)3	1.19	3.54	0.268	1.13	12
N(Ph-3T-DCV-Ph)3	1.08	3.71	0.283	1.13	12
SubNc	1.1	2.10	0.23	0.60	13
SubPc	1.02	2.70	0.28	0.80	13
BDHT	1.14	0.07	0.24	0.03	14
DTDCPB	1.05	1.42	0.33	0.49	15

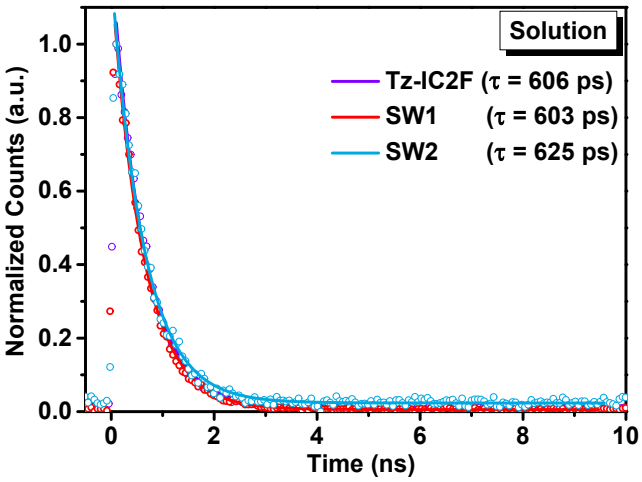

Figure S12. Time-resolved PL signals of Tz-IC2F, SW1, and SW2 in dilute CF solutions.

Table S8. Transient PL fit parameters of the Tz-IC2F, SW1 and SW2 by single-exponential function in chloroform function (~10-5 M). The solution samples were excited at 400 nm and probed at 770 nm.

Sample	A_1	τ_1 (ps)
Tz-IC2F	1.23	606
SW1	1.19	603
SW2	1.17	625

Table S9. Transient PL fit parameters by biexponential function for Tz-IC2F, SW1 and SW2 film. The film samples were excited at 400 nm and probed at 860 nm.

Sample	A_1	τ_1 (ps)	A_2	τ_2 (ps)	τ_{avg} [a] (ps)
Tz-IC2F	0.578	556	0.578	556	556
SW1	3.74	71	0.18	315	82
SW2	0.49	298	2.02	96	135

[a]The average lifetime values were extracted by a biexponential function fit and calculated according to the equation: $\tau_{avg} = \sum_i A_i\tau_i / \sum_i A_i$.

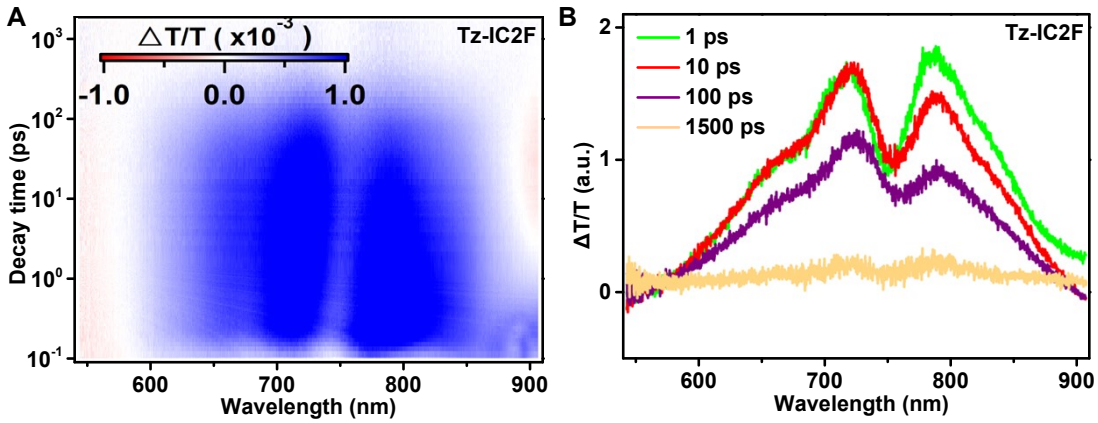

Figure S13. (A) 2D transient absorption map of Tz-IC2F pumped at 750 nm and (B) the corresponding spectrum at several delay times (probe pulse at 1 ps, 10 ps, 100 ps and 1000 ps delay times.

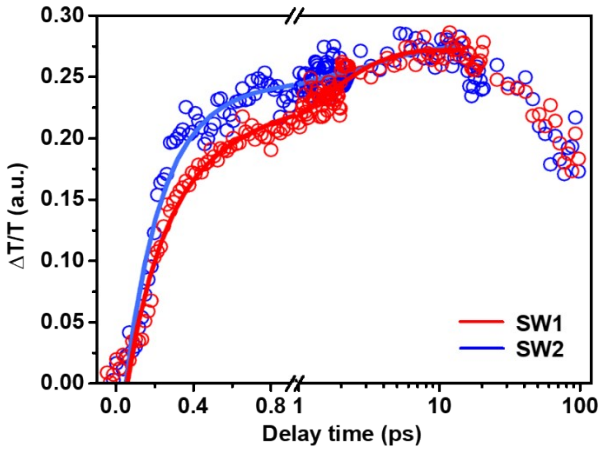

Figure S14. TA kinetics of SW1 and SW2 GSB.

Table S10. Detailed parameters of TA spectra, the hole transfer kinetics were fitted by a biexponential function: $i = A_1 \exp(-t/\tau_1) + A_2 \exp(-t/\tau_2)$, with two lifetimes of τ_1 and τ_2 and prefactors of A_1 and A_2.

Sample	A_1	τ_1 (ps)	A_2	τ_2 (ps)	HF lifetime (ps)
SW1	13.7%	0.23 ± 0.02	86.3%	3.52 ± 0.35	3.07 ± 0.30
SW2	35.7%	0.24 ± 0.02	64.3%	2.10 ± 0.21	1.44 ± 0.14

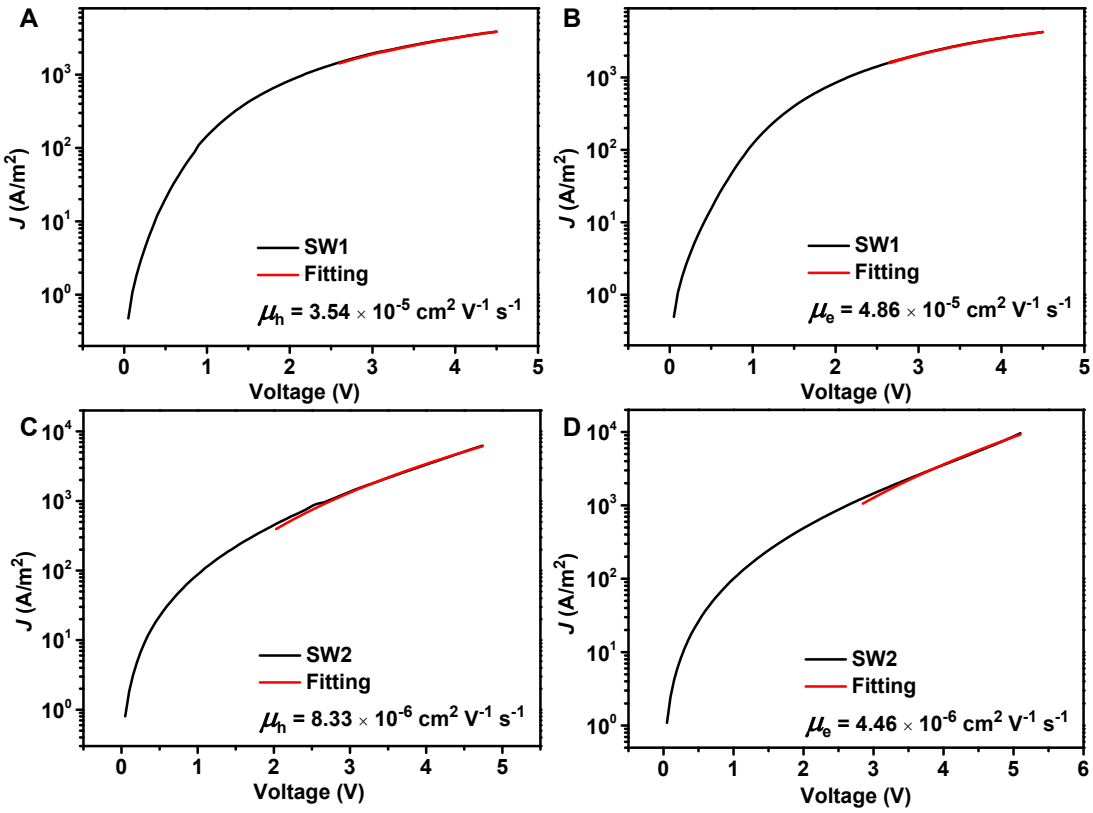

Figure S15. The SCLC curves of (A) SW1 and (C) SW2 based on hole-only devices and (B) SW1, (D) SW2 based electron-only devices. The inset mobility data are average values of eight films.

3. NMR spectra

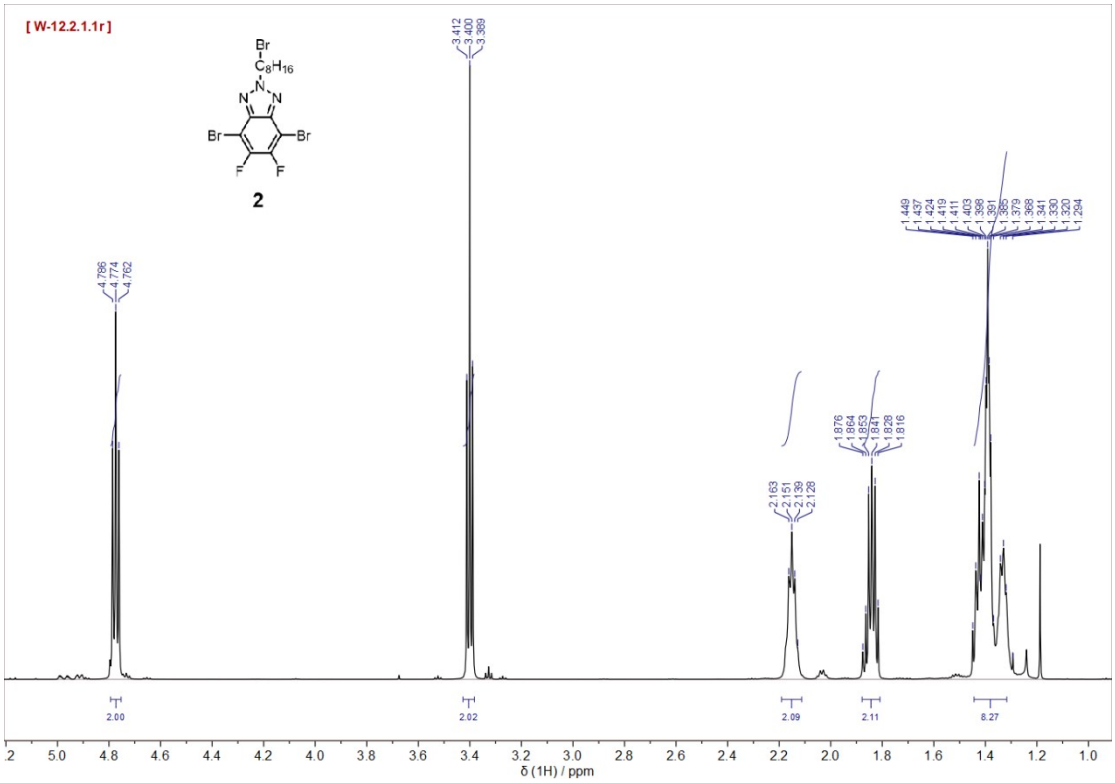

Figure S16. ^{1}H-NMR spectrum of compound 2.

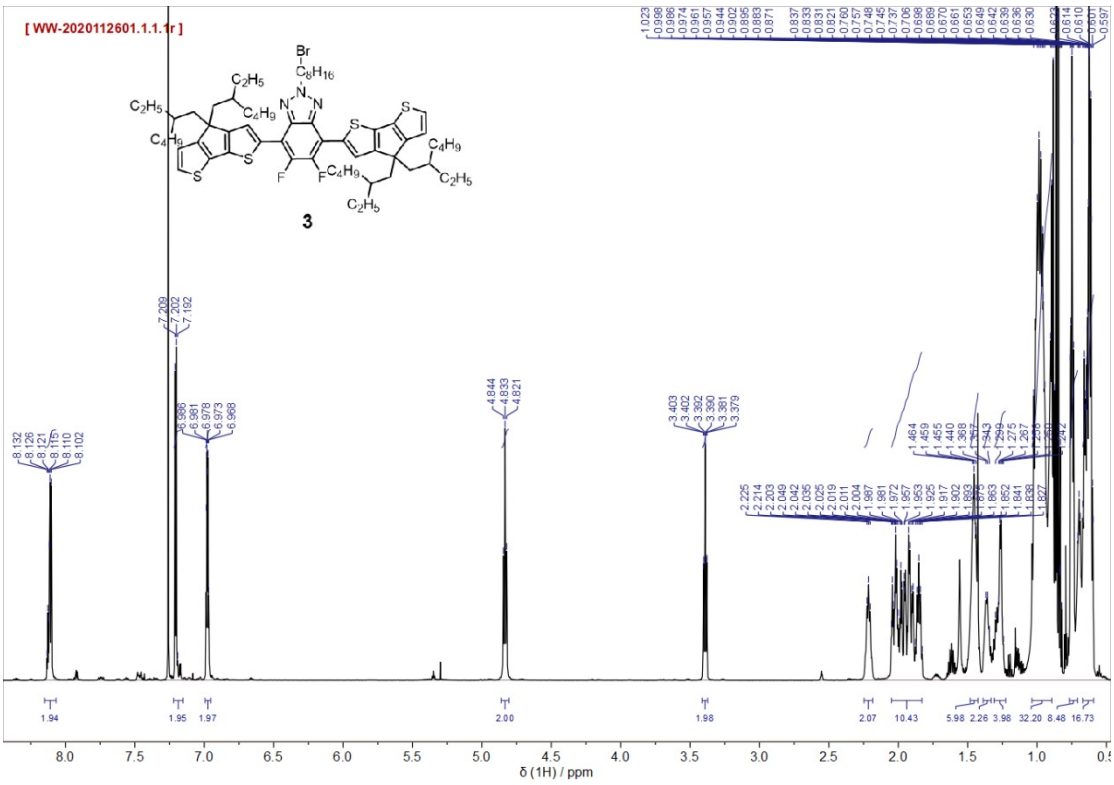

Figure S17. ^{1}H-NMR spectrum of compound 3.

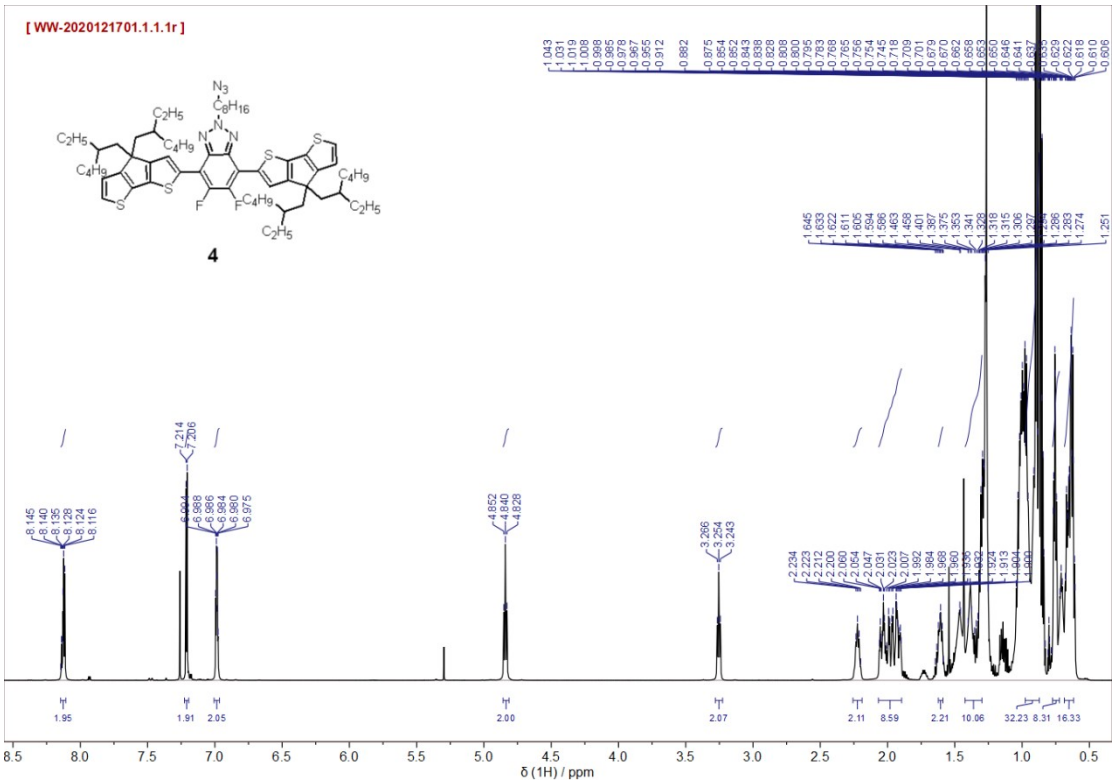

Figure S18. ^{1}H-NMR spectrum of compound 4.

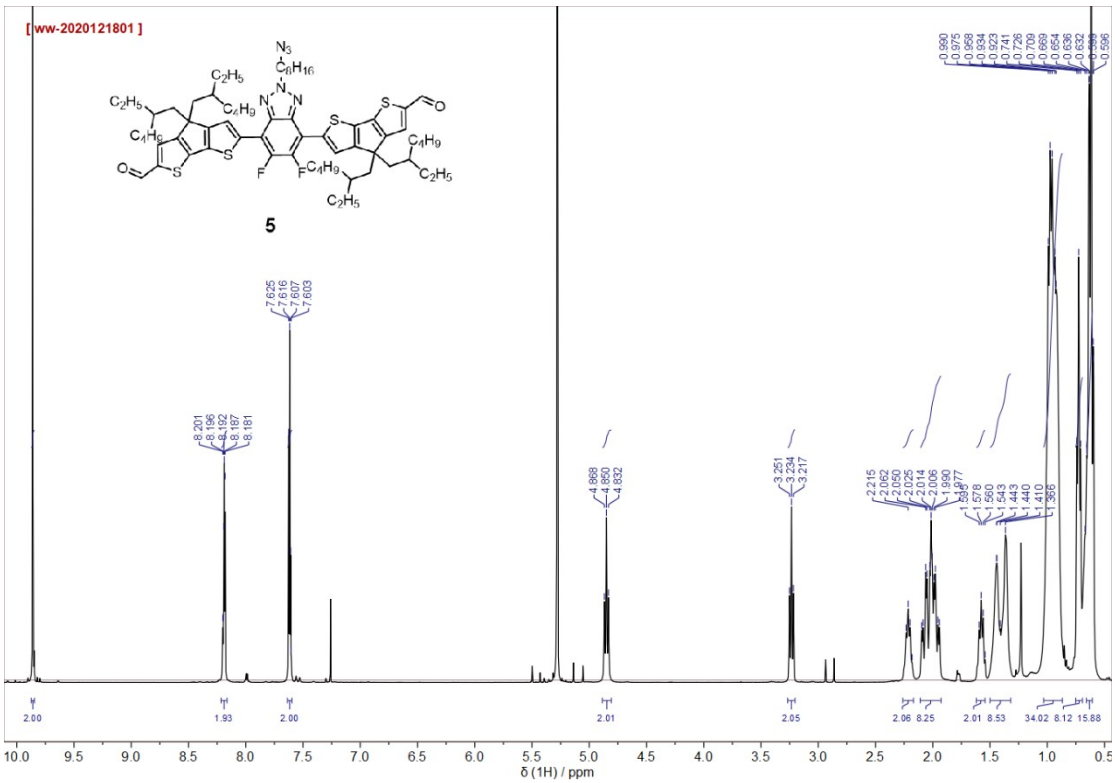

Figure S19. ^{1}H-NMR spectrum of compound 5.

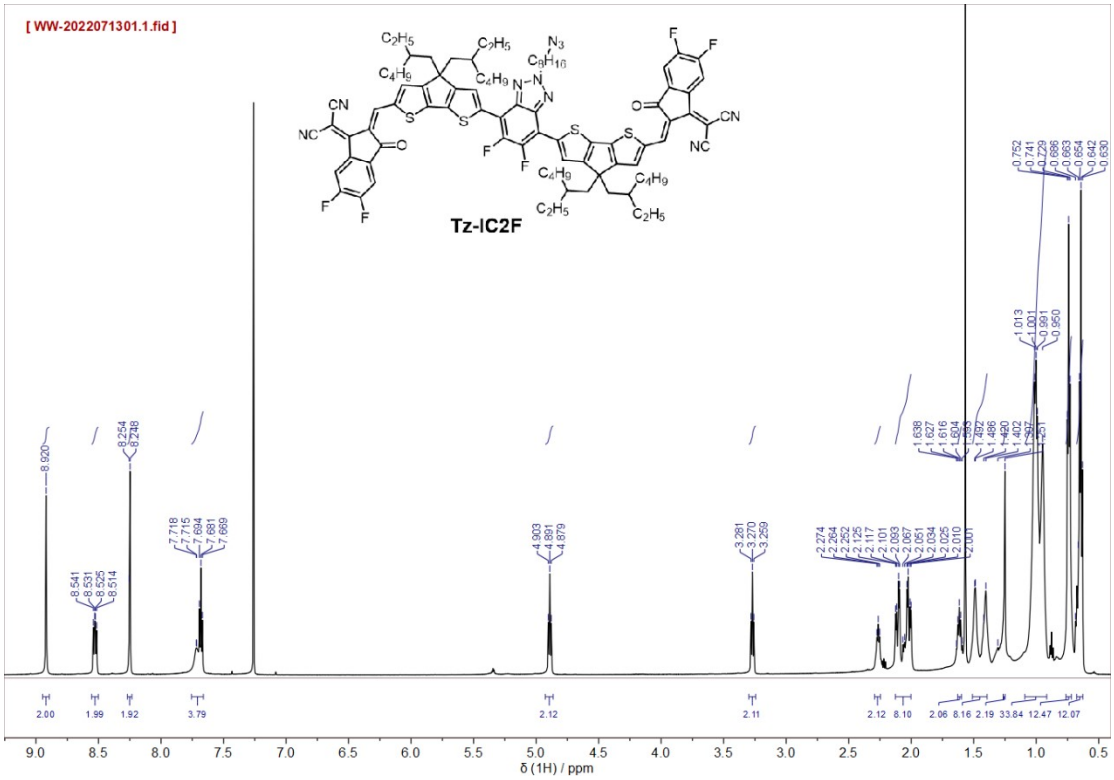

Figure S20. ^{1}H-NMR spectrum of Tz-IC2F.

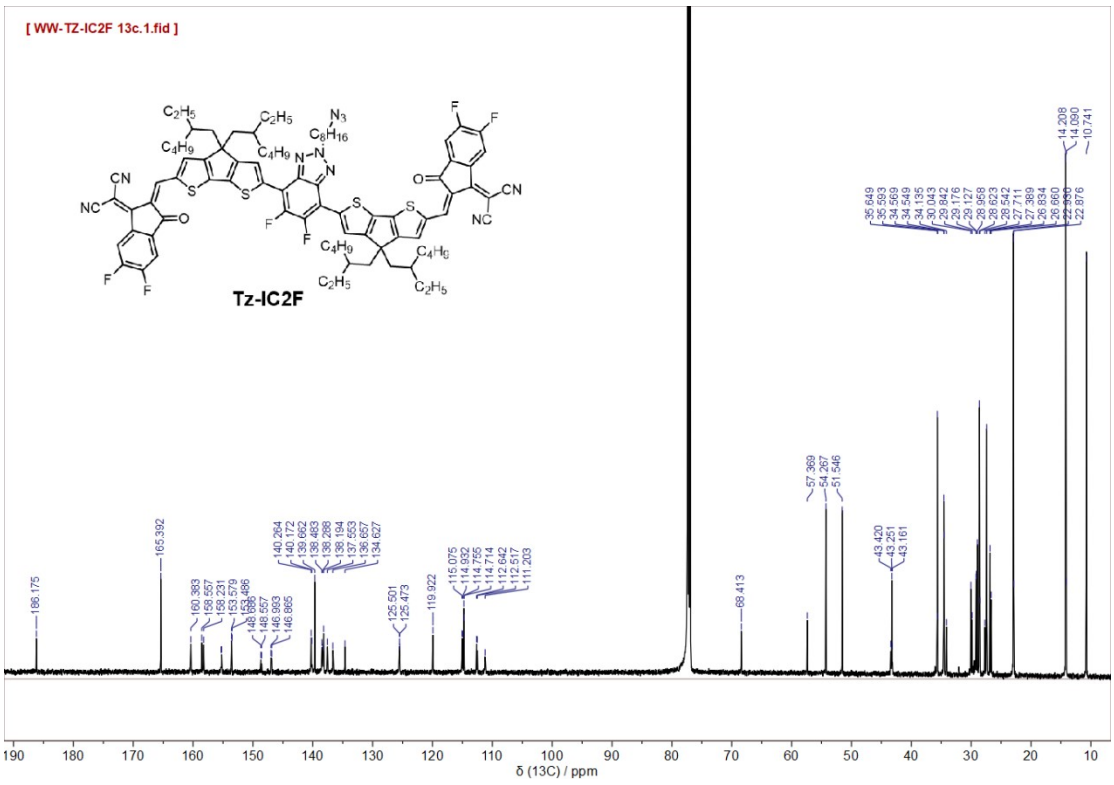

Figure S21. ^{13}C-NMR spectrum of Tz-IC2F.

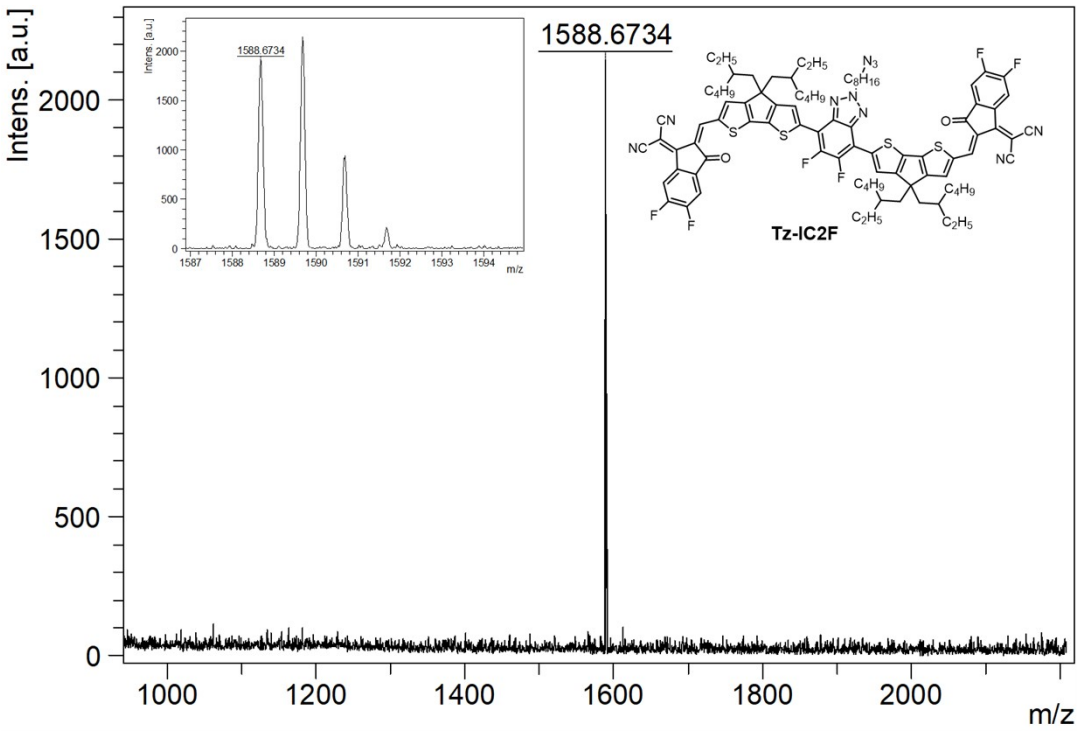

Figure S22. Mass spectrum of *Tz-IC2F*.

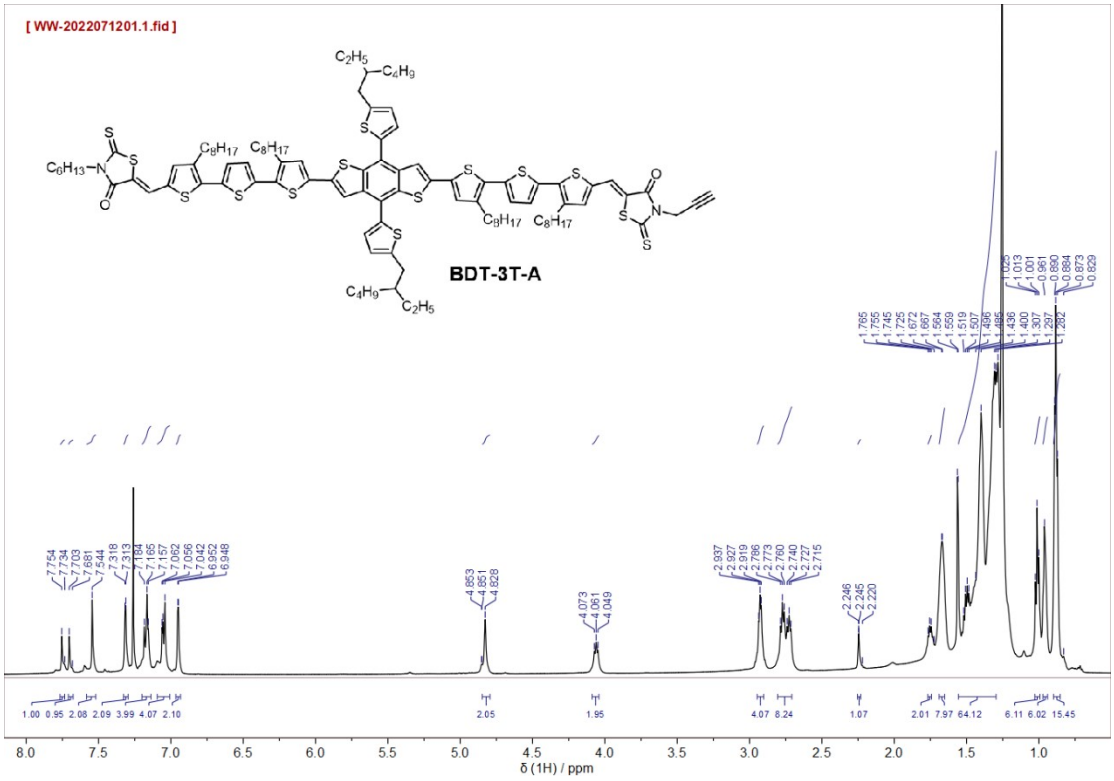

Figure S23. ^{1}H-NMR spectrum of BDT-3T-A.

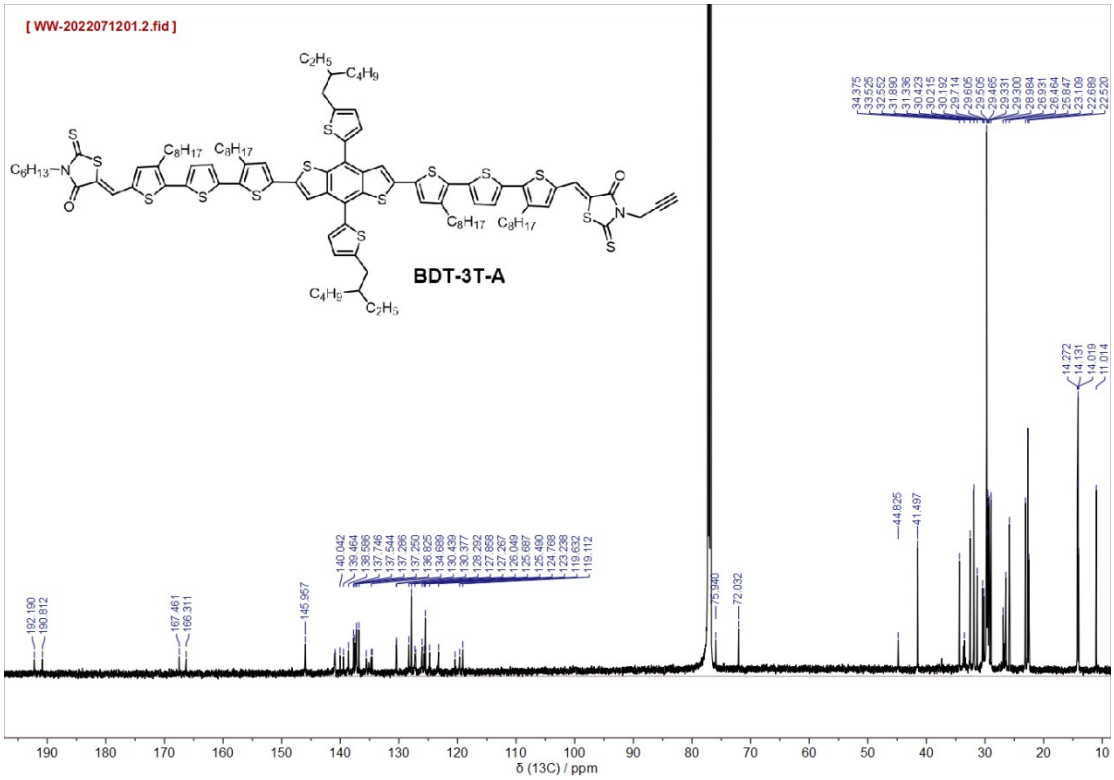

Figure S24. ^{13}C-NMR spectrum of BDT-3T-A.

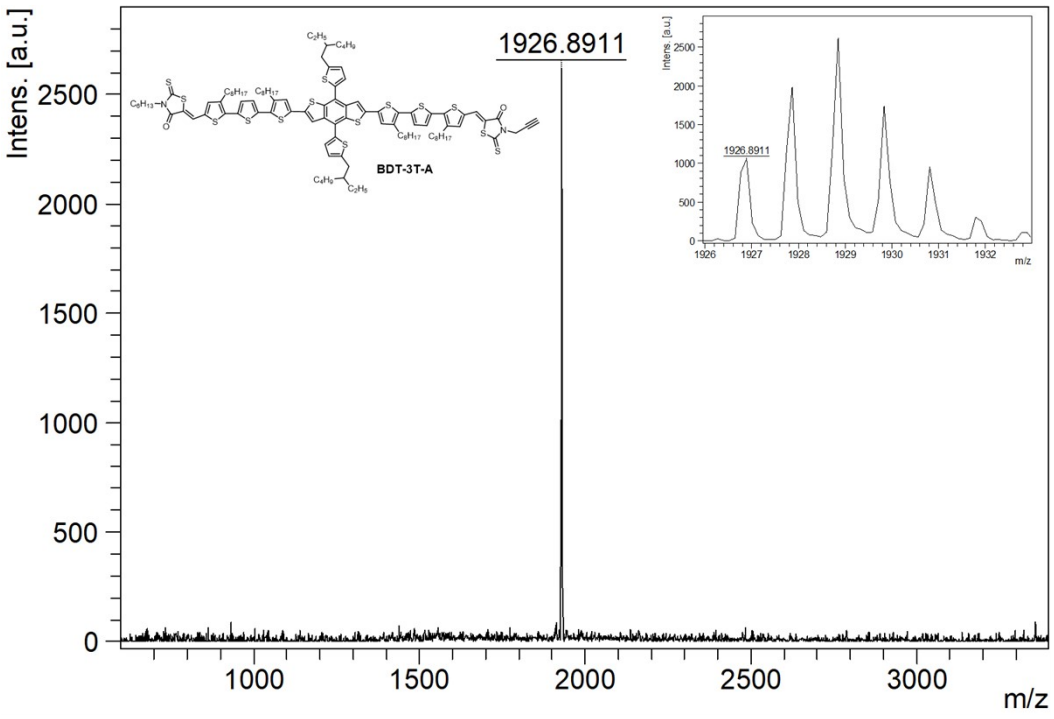

Figure S25. Mass spectrum of *BDT-3T-A*.

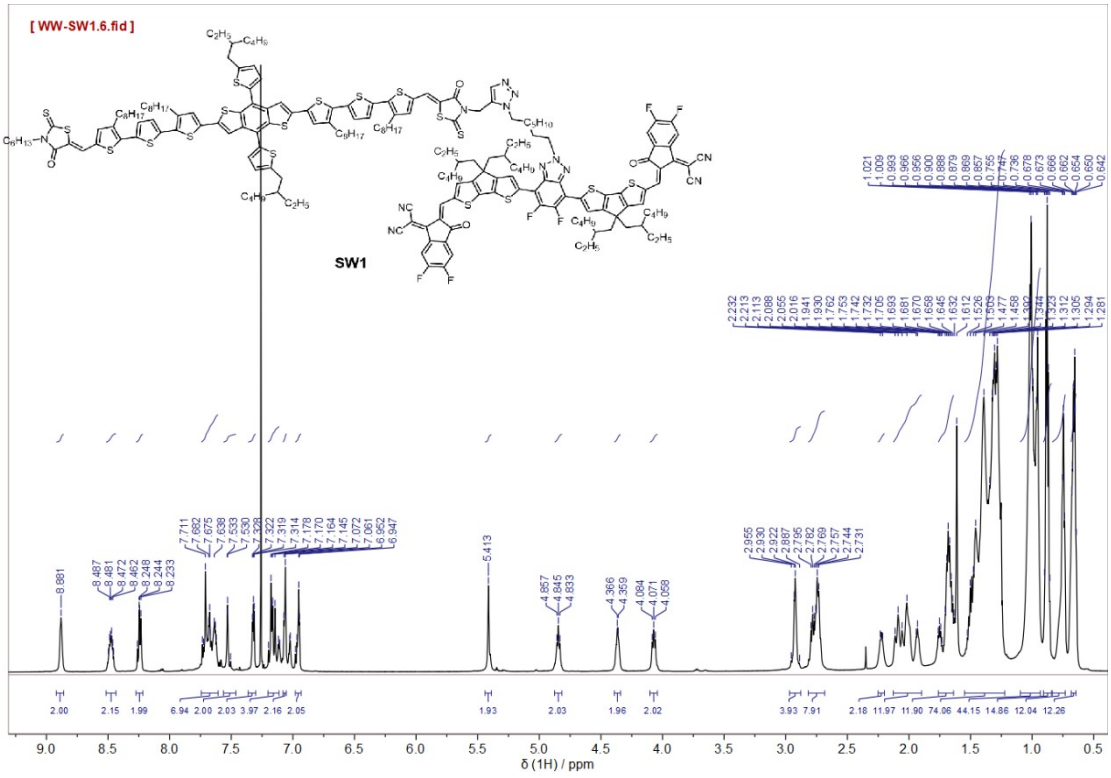

Figure S26. ^{1}H-NMR spectrum of SW1.

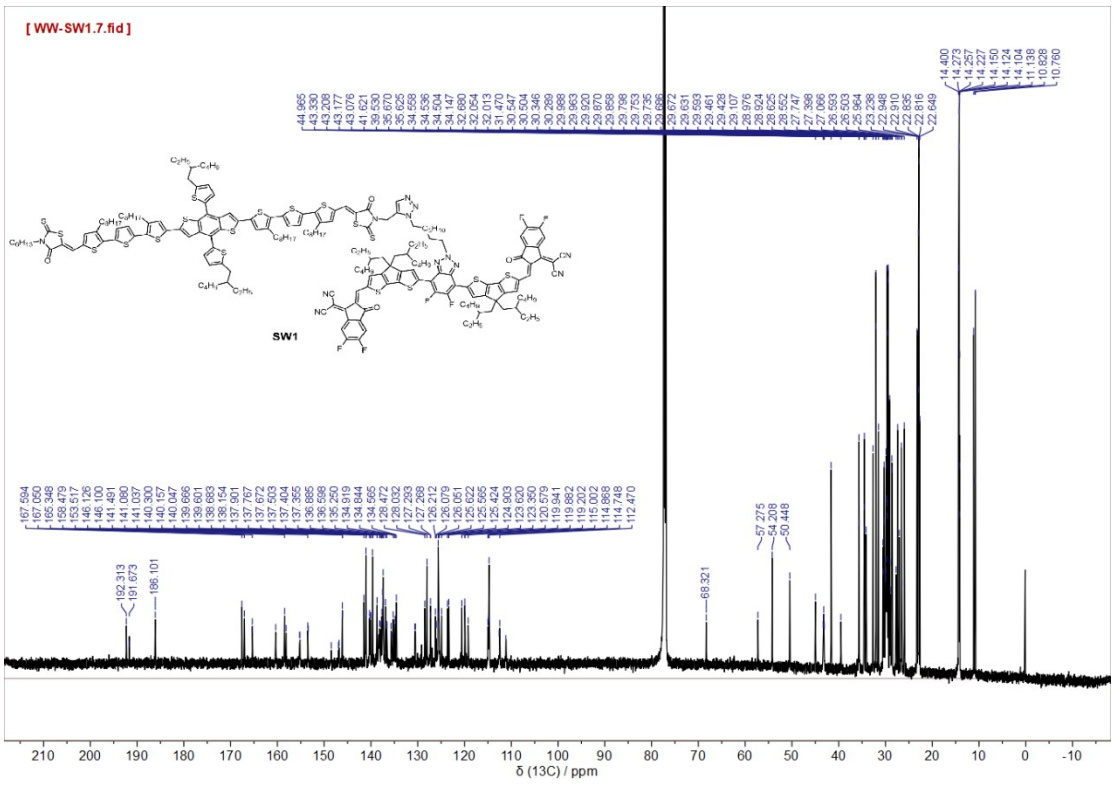

Figure S27. ^{13}C-NMR spectrum of SW1.

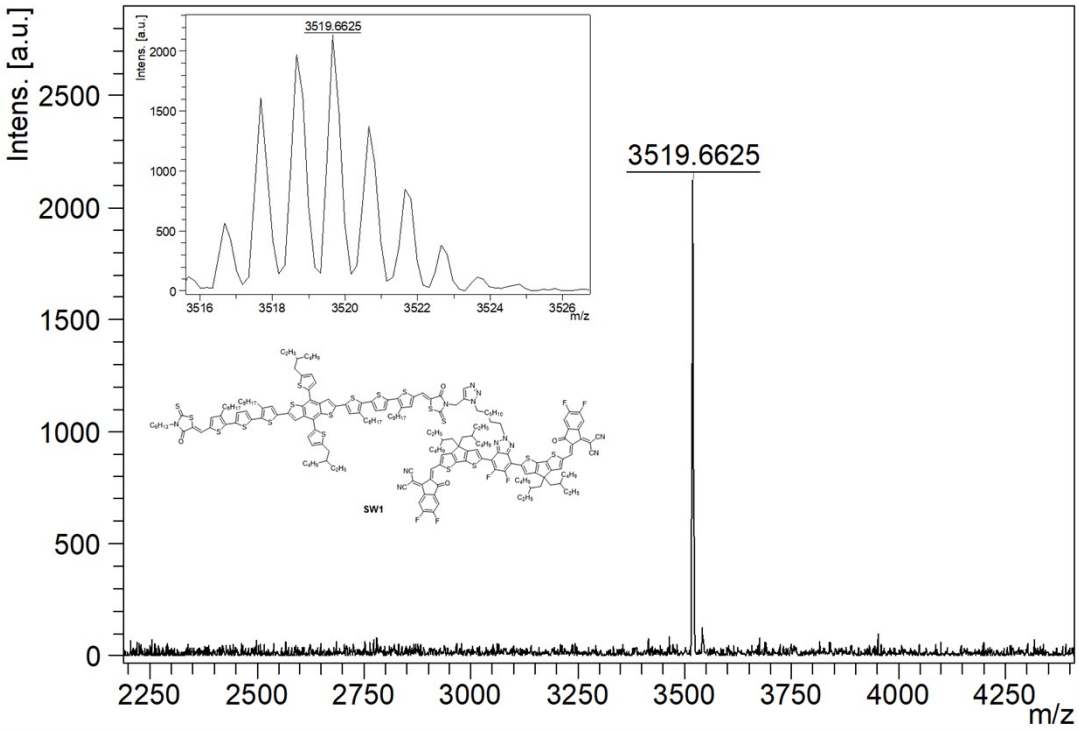

Figure S28. Mass spectrum of *SW1*.I

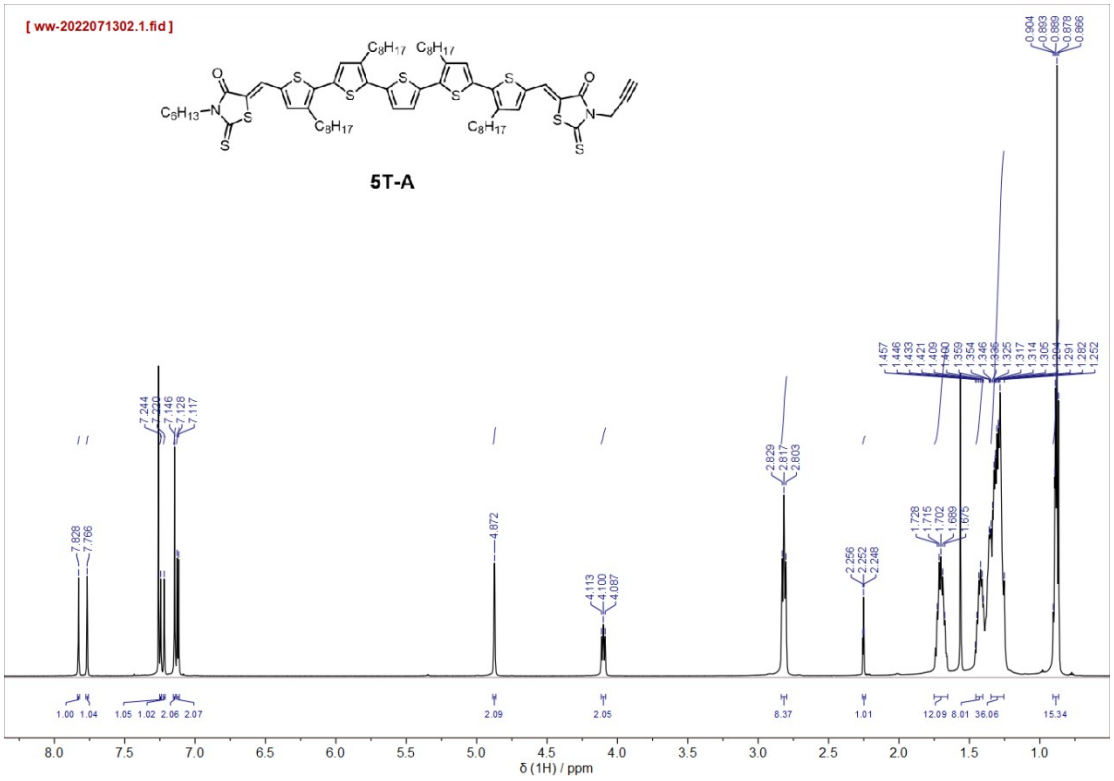

Figure S29. ^{1}H-NMR spectrum of 5T-A.

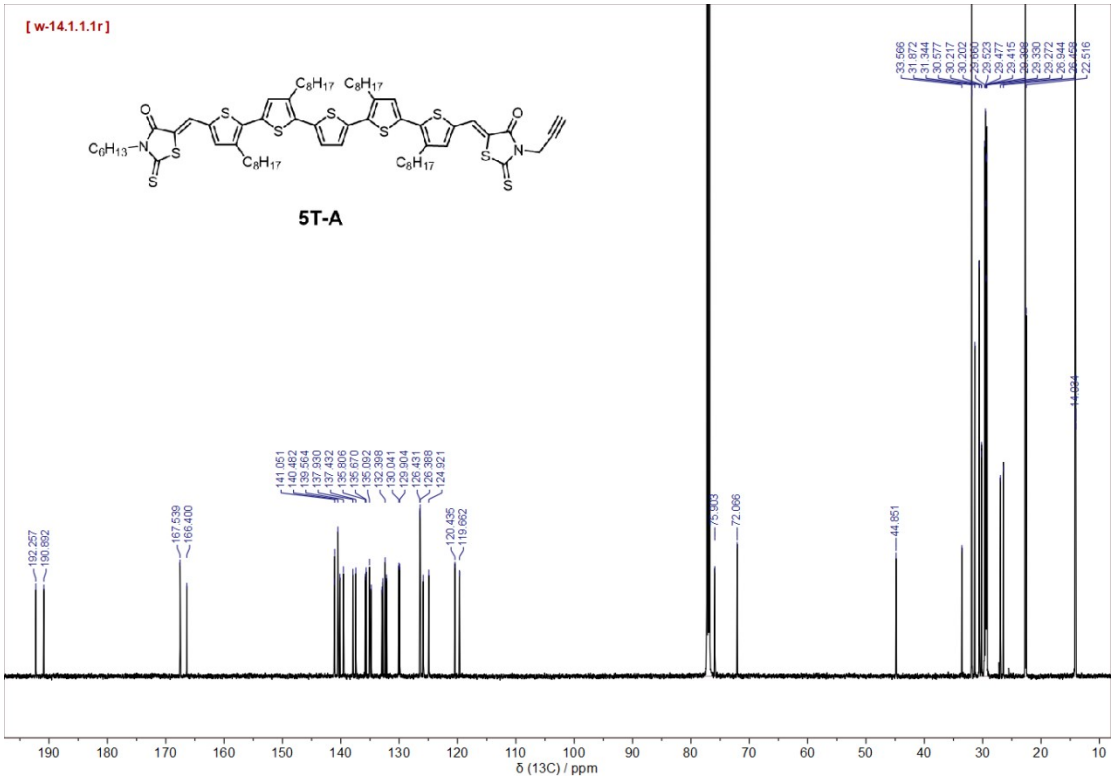

Figure S30. ^{13}C-NMR spectrum of 5T-A.

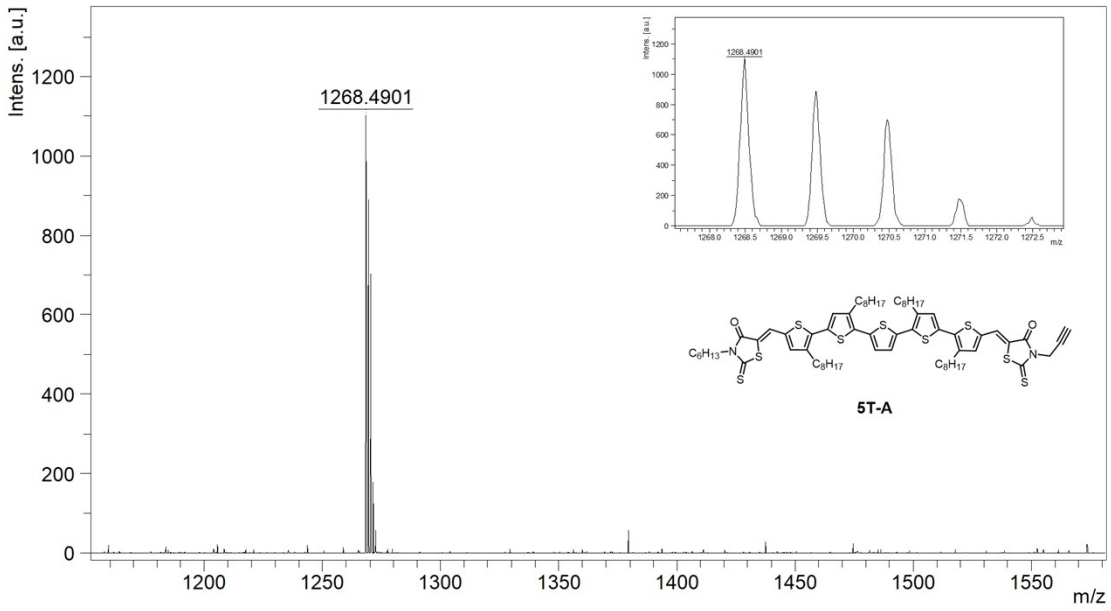

Figure S31. Mass spectrum of *5T-A*.

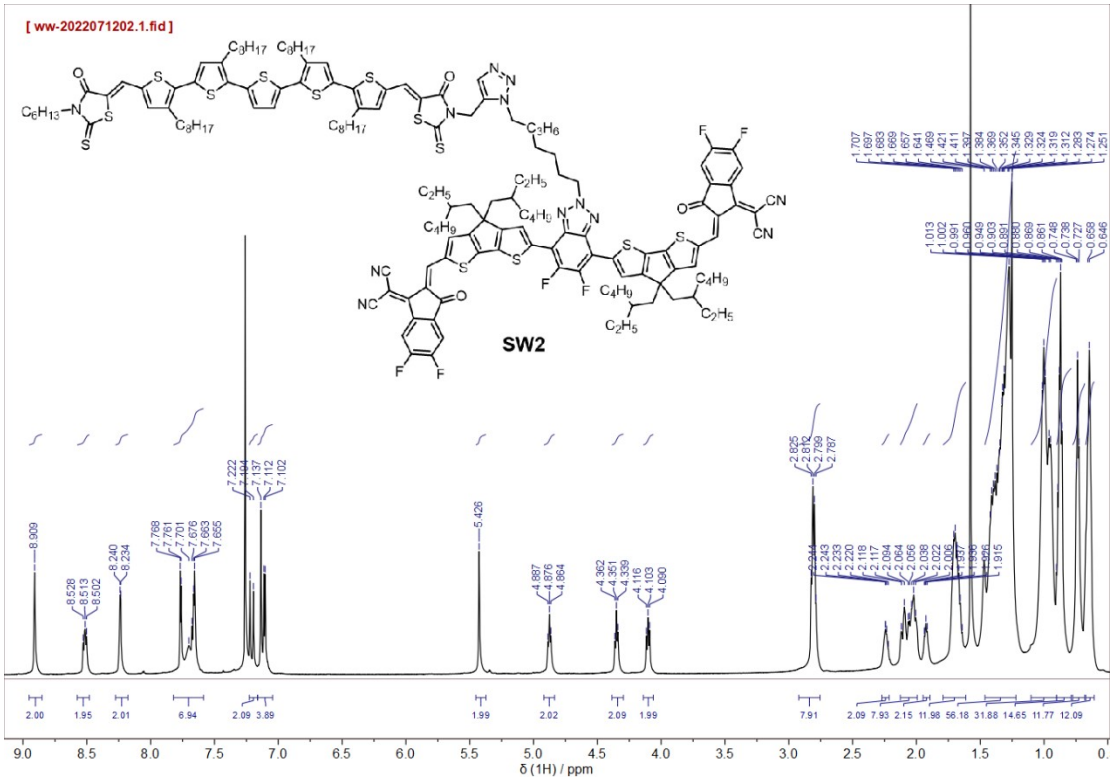

Figure S32. ^{1}H-NMR spectrum of SW2.

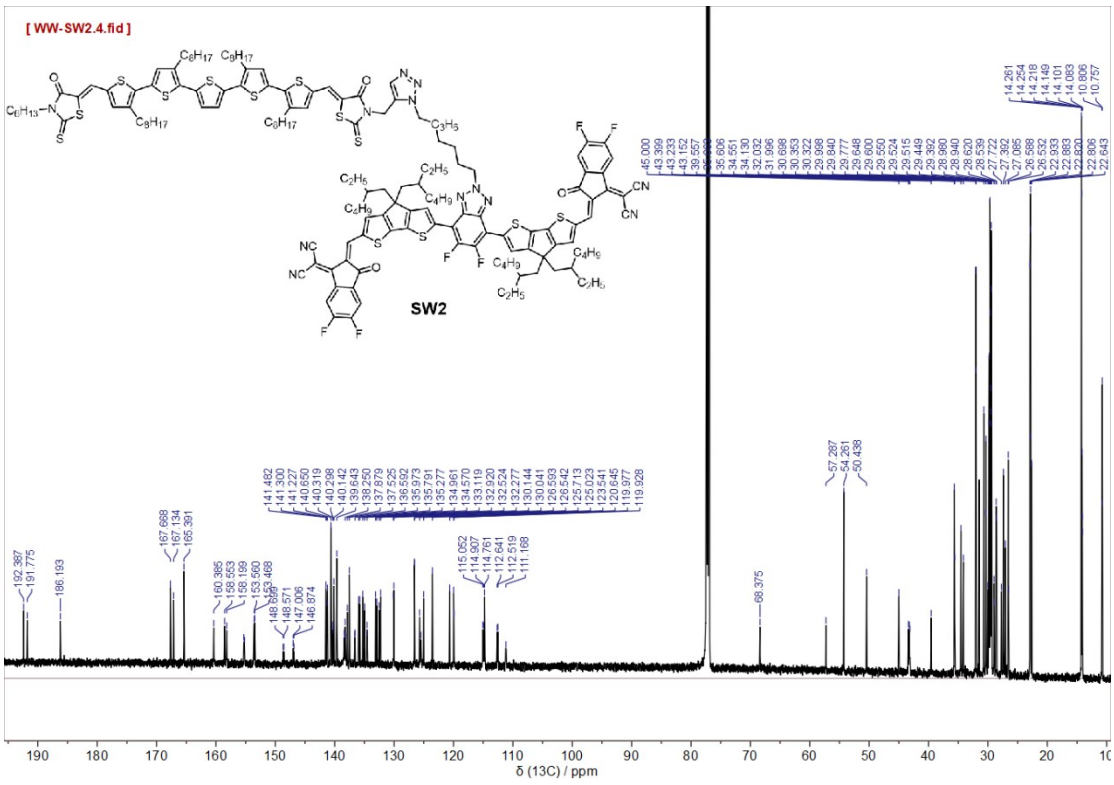

Figure S33. ^{13}C-NMR spectrum of SW2.

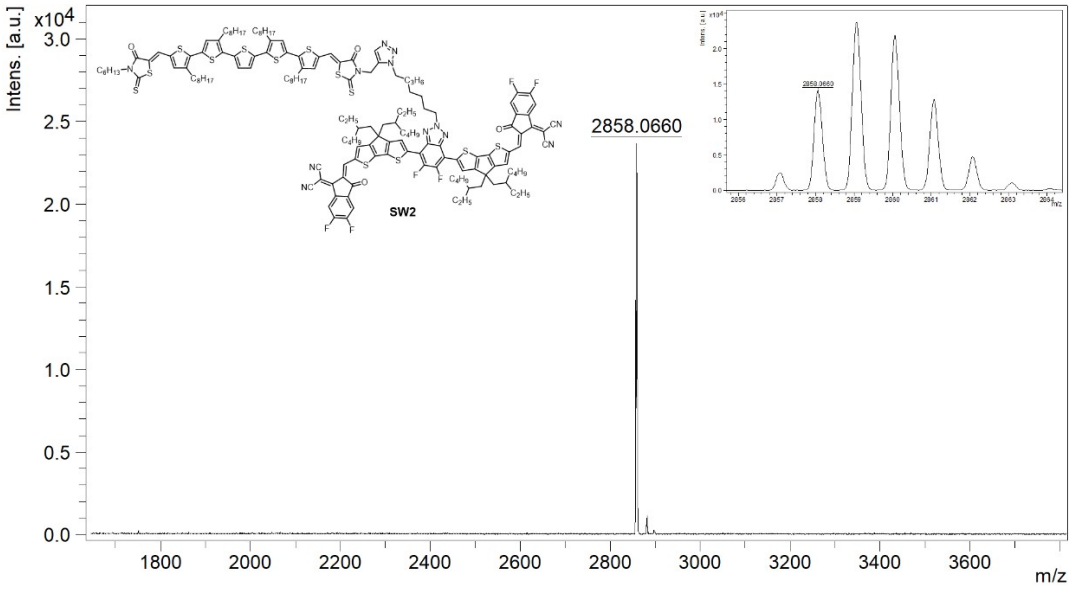

Figure S34. Mass spectrum of *SW2***.**

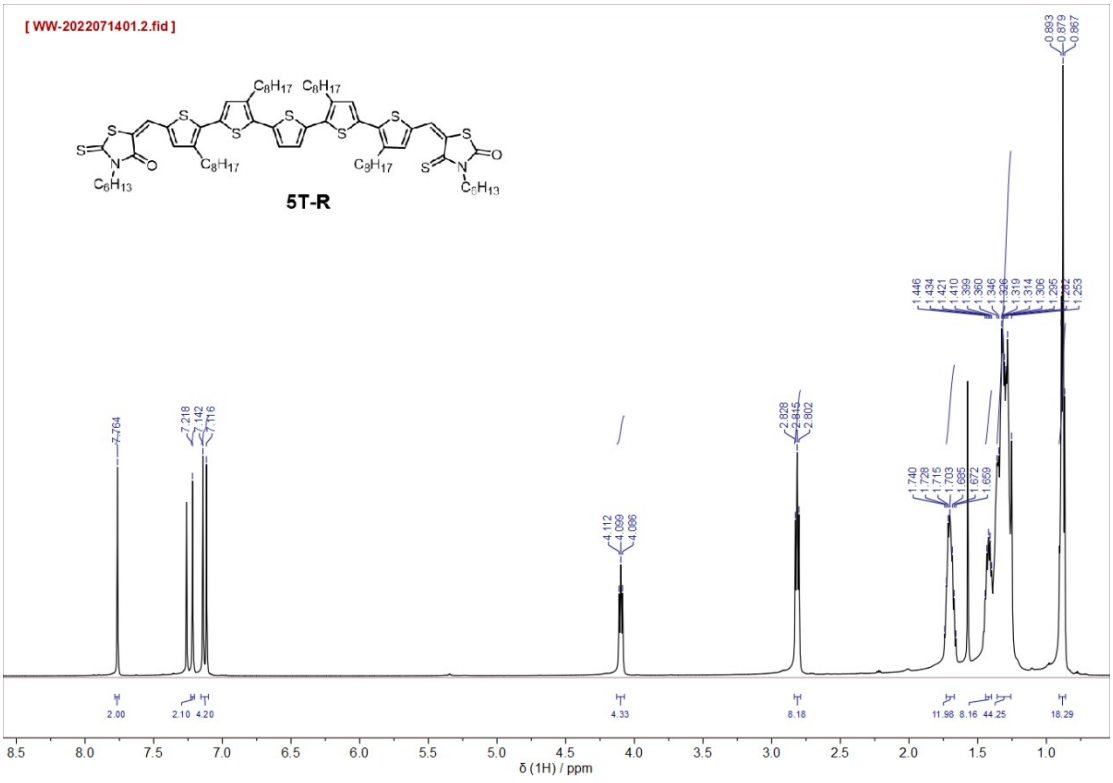

Figure S35. ^{1}H-NMR spectrum of 5T-R.

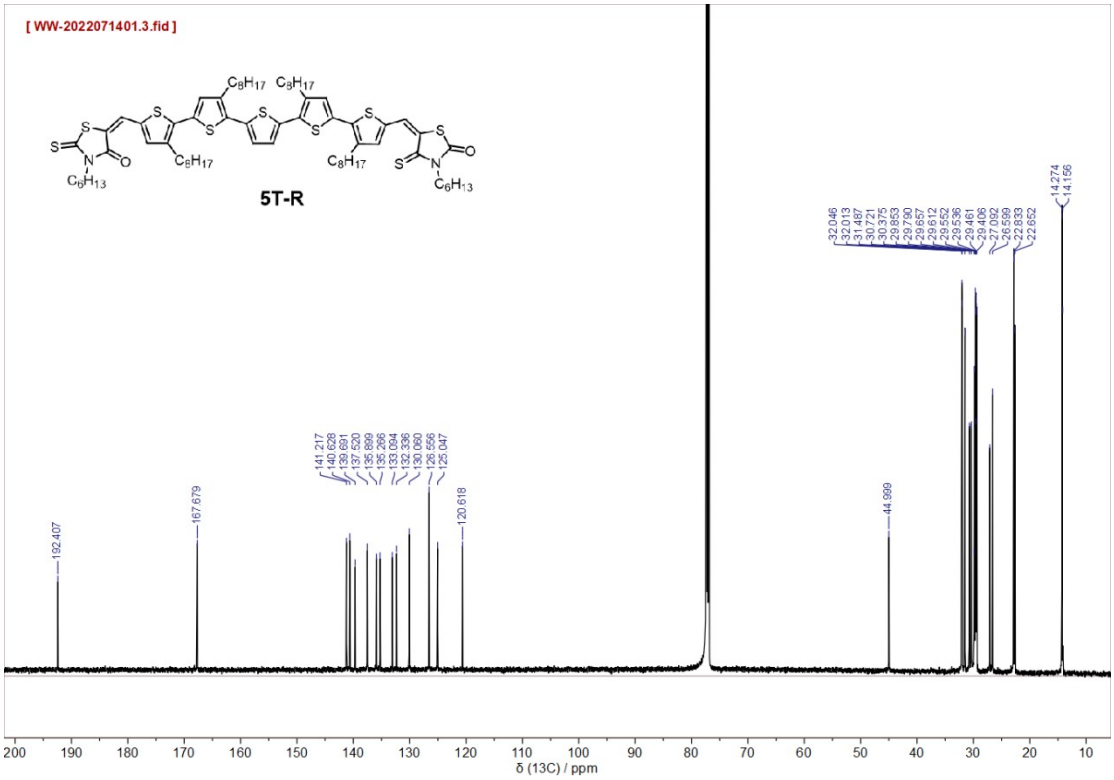

Figure S36. ^{13}C-NMR spectrum of 5T-R.

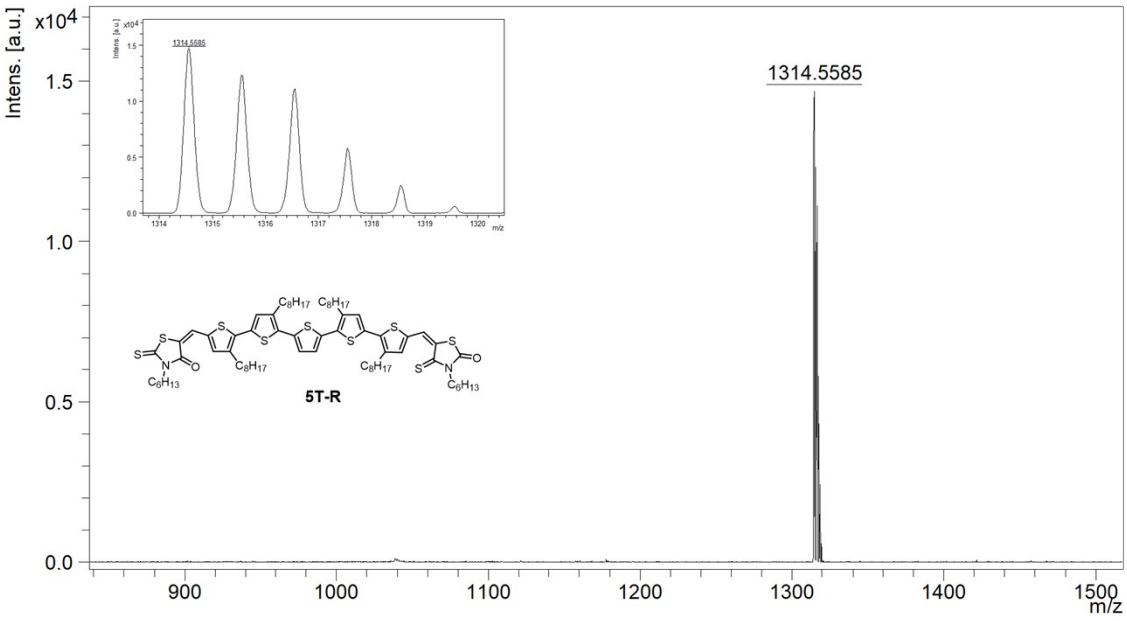

Figure S37. Mass spectrum of *5T-R*.

4. References

1 Sun, R.; Wu, Y.; Guo, J.; Luo, Z.; Yang, C.; Min, J. *Sci. China Chem.* **2020**, *63*, 1246.

2 Cravino, A.; Leriche, P.; Alévêque, O.; Roquet, S.; Roncali, J. *Adv. Mater.* **2006**, *18*, 3033.

3 Bu, L.; Guo, X.; Yu, B.; Qu, Y.; Xie, Z.; Yan, D.; Geng, Y.; Wang, F. *J. Am. Chem. Soc.* **2009**, *131*, 13242.

4 Bu, L.; Guo, X.; Yu, B.; Fu, Y.; Qu, Y.; Xie, Z.; Yan, D.; Geng, Y.; Wang, F. *Polymer* **2011**, *52*, 4253.

5 Qu, J.; Gao, B.; Tian, H.; Zhang, X.; Wang, Y.; Xie, Z.; Wang, H.; Geng, Y.; Wang, F. *J. Mater. Chem. A* **2014**, *2*, 3632.

6 Izawa, S.; Nishizawa, T.; Hashimoto, K.; Koganezawa, T.; Tajima, K. *Synthetic Met.* **2014**, *197*, 175.

7 Di Maria, F.; Biasiucci, M.; Di Nicola, F. P.; Fabiano, E.; Zanelli, A.; Gazzano, M.; Salatelli, E.; Lanzi, M.; Della Sala, F.; Gigli, G.; Barbarella, G. *J. Phys. Chem. C.* **2015**, *119*, 27200.

8 Xia, D.; Yang, F.; Li, J.; Li, C.; Li, W. *Mater. Chem. Front.* **2019**, *3*, 1565.

9 Zhang, Y.; Deng, D.; Wu, Q.; Mi, Y.; Yang, C.; Zhang, X.; Yang, Y.; Zou, W.; Zhang, J.; Zhu, L.; Zhou, H.; Liu, X.; Wei, Z. *Sol.RRL* **2020**, *4*, 1900580.

10 Liu, X.; Xie, B.; Duan, C.; Wang, Z.; Fan, B.; Zhang, K.; Lin, B.; Colberts, F. J. M.; Ma, W.; Janssen, R. A. J.; Huang, F.; Cao, Y. *J. Mater. Chem. A* **2018**, *6*, 395.

11 Solodukhin, A. N.; Luponosov, Y. N.; Mannanov, A. L.; Savchenko, P. S.; Bakirov, A. V.; Shcherbina, M. A.; Chvalun, S. N.; Paraschuk, D. Y.; Ponomarenko, S. A. *Energies* **2021**, *14*, 3596.

12 Mannanov, A. L.; Savchenko, P. S.; Luponosov, Y. N.; Solodukhin, A. N.; Ponomarenko, S. A.; Paraschuk, D. Y. *Org. Electron.* **2020**, *78*, 105588.

13 Chandran, H. T.; Ng, T. W.; Foo, Y.; Li, H. W.; Qing, J.; Liu, X. K.; Chan, C. Y.; Wong, F. L.; Zapien, J. A.; Tsang, S. W.; Lo, M. F.; Lee, C. S. *Adv. Mater.* **2017**, *29*, 1606909.

14 Sun, X.; Liu, Y.; Xu, X.; Yang, C.; Yu, G.; Chen, S.; Zhao, Z.; Qiu, W.; Li, Y.; Daoben, Z. *J. Phys. Chem. B* **2005**, *109*, 10789.

15 Nakayama, K. I.; Okura, T.; Okuda, Y.; Matsui, J.; Masuhara, A.; Yoshida, T.;

White, M. S.; Yumusak, C.; Stadler, P.; Scharber, M.; Sariciftci, N. S. *Materials (Basel)* **2021**, *14*, 120**.**